Journal of
Marine Science and Engineering

MDPI

Article

Decreasing Vulnerability of Storm Surge Disasters in Coastal Cities of China over the Past 30 Years

Dan Meng [1,2], Yueming Liu [1,2], Zhihua Wang [1,2], Xiaomei Yang [1,2,*], Xiaoliang Liu [1,2], Junyao Zhang [1,2] and Ku Gao [1,2]

1 State Key Laboratory of Resources and Environmental Information System, Institute of Geographic Sciences and Natural Resources Research, Chinese Academy of Sciences, Beijing 100101, China
2 University of Chinese Academy of Sciences, Beijing 100049, China
* Correspondence: yangxm@lreis.ac.cn; Tel.: +86-13671241172

Abstract: From 2000 to 2020, storm surges occurred 397 times in China, resulting in direct economic losses of up to CNY 220.64 billion. Storm surges not only threaten safety but also cause property damage; hence, it is necessary to assess the changes in vulnerability to storm surges in order to understand how to reduce said vulnerability. Fifteen coastal cities of four types were chosen, with different levels of urban development, rapid expansion of impervious surface, high extent of agricultural land, and high fishery output value. Viewing vulnerability through the dimensions of exposure, sensitivity, and adaptability, a GIS and RS were used to evaluate and assess the vulnerability in 15 coastal cities in China over the past 30 years. The results indicated that the vulnerability of these 15 Chinese cities presented the characteristics of a continuous downward trend from 1990 to 2020, and the average rate of reduction in vulnerability over the 10 years from 2005 to 2015 was the highest, at 2.23%. The areas of high vulnerability shifted from the southern region to the northern region. The vulnerabilities in the southern region, with Shanghai, Shenzhen, and Dongguan, changed significantly, to 3.30%, 3.20%, and 3.45%, respectively. An important factor in determining vulnerability reductions is a city's ability to adapt to storm surges. Coastal cities can improve their adaptability to storm surge disasters through general public budget expenditure, investment in fixed assets, GDP, and medical and health services, thereby alleviating their vulnerability. Due to China's frequent storm surge disasters during the 2005–2015 period, government departments have strengthened the investment of relevant resources in adaptive indicators, ultimately causing the cities' vulnerability to rapidly decrease during this period.

Keywords: vulnerability; spatiotemporal change; China; coastal zone; adaptability; disaster mitigation; storm surge

Citation: Meng, D.; Liu, Y.; Wang, Z.; Yang, X.; Liu, X.; Zhang, J.; Gao, K. Decreasing Vulnerability of Storm Surge Disasters in Coastal Cities of China over the Past 30 Years. *J. Mar. Sci. Eng.* **2023**, *11*, 128. https://doi.org/10.3390/jmse11010128

Academic Editors: Felice D'Alessandro and Chunyan Li

Received: 16 November 2022
Revised: 29 December 2022
Accepted: 4 January 2023
Published: 6 January 2023

1. Introduction

Coastal areas are important for socioeconomic development in coastal countries and feature the most energetic and frequent human activities. Coastal areas are the junction of land and sea, with complex and multilateral natural environments. Furthermore, coastal areas are key areas in which natural disasters frequently occur [1,2]. In the context of global warming, frequent storm surges—such as typhoons and floods—increase the risk of natural disasters in coastal regions. How to reduce and prevent disasters has long been a focus of national attention. As defined by the United Nations Development Programme (2005), natural disaster risks are the result of the interaction between human or naturally induced vulnerabilities and disasters, with a probability of harmful impacts (i.e., economic, infrastructural, and/or environmental) occurring. Storm surges lead to frequent disasters in coastal areas, and their regularity is difficult to control. Reducing the vulnerability of coastal areas is the most direct and effective way to reduce losses caused by disasters [3]. The concept of vulnerability, as defined by the IPCC, is "the tendency to be adversely affected, the various concepts and factors of vulnerability, the sensitivity or susceptibility to harm, and the lack of coping and adaptation ability". Based on the understanding of the concept of vulnerability presented by the IPCC, vulnerability, in this paper, is understood to be composed of three aspects: the degree of exposure of areas susceptible to adverse external environments, and the sensitivity and adaptability of human activities to external stimuli when coastal areas are exposed to adverse environments. There has been a trend of considering coastal regional vulnerability, and of strengthening the effective management of the sustainable development of vulnerable areas, when conducting storm surge risk research.

As our understanding of coastal vulnerability to storm surges in China is lacking, more research is urgently needed. China's coastal region is one of the major typhoon-prone areas of the world. It is located in the northwestern margin of the northwest Pacific storm basin, which is the largest tropical storm region in the world, and 36% of the total number of typhoons originate from this area [4]. Additionally, coastal areas in China are important population and economic centers and are among the core hotspots for global economic development [5]. The occurrence of recorded events of storm surge disasters has risen sharply, resulting in tremendous economic losses in China and the world. The "14th Five-Year Plan" National Comprehensive Disaster Prevention and Mitigation Plan, issued by China, noted that the vulnerability of various disaster-bearing bodies is increasing. The plan further indicated that there are great shortcomings and deficiencies in mitigation when facing complicated and severe forms of natural disasters [6]. For that reason, assessing vulnerability to storm surges can provide scientific support and a decision-making basis for China's risk prevention and mitigation.

According to current research on vulnerability in China, the focus is on both the spatial distribution characteristics and the driving force factors. This is based on a comprehensive vulnerability assessment model used to calculate the coastal vulnerability index and generate a vulnerability level distribution map to determine the spatial distribution characteristics of vulnerability [7]. The results show that high-vulnerability areas are concentrated in areas with a higher disaster frequency, higher population density, higher GDP, and higher proportion of both built-up and cropland areas, along with low-lying coastal areas with flat terrain and physical structures without topographic barriers [8–15]. The above studies providing a vulnerability evaluation in China have mainly focused on the exposure and sensitivity aspects, while neglecting the mitigation of vulnerability caused by storm surge disasters in coastal areas. In another study, considering mitigation indicators such as seawalls, the results showed that most coastal areas with rapid urbanization lack high-level seawalls and have insufficient resistance [16,17]. Although the above studies have considered adaptability indicators, the impact of mitigation ability is still at a single-period static spatial level, and we do not know the trend of spatiotemporal changes in coastal vulnerability. Furthermore, with the continuing influx of large numbers of people into coastal regions, human stresses on the coastal ecosystem and resources are growing, while at the same time climate variability, climate change, and associated changes in the marine environment are leading to unoptimistic tendencies regarding the vulnerability of coastal areas [18]. Based on this, this study argues that assessing the vulnerability of coastal areas should not only focus on the spatial level, but also focus on the spatiotemporal changes in vulnerability.

There are existing studies that have analyzed the spatiotemporal changes in China's coasts, provinces, and cities. Different trends in vulnerability correspond to varied factors that affect vulnerability. Li CW et al. used catastrophe theory to fully integrate water, heat, and vegetation biodiversity, as complex exposure indicators, into urban vulnerability analysis, revealing that coastal cities in China were exposed to natural biophysical processes in the past 20 years, from 2000 to 2020, and the results showed that the vulnerability of China's coastal areas is generally on the rise [19]. Zhou YF et al. analyzed the landscape vulnerability changes and spatiotemporal evolution rules that were affected by human activities in Jiangsu Province from 2000 to 2015 by constructing a spatiotemporal relationship evaluation model of landscape vulnerability in counties in Jiangsu Province, and the results showed that the landscape vulnerability of counties with high human activity intensity is increasing [20]. Yu HM et al. explored the change law of social vulnerability in Shenzhen from 1986 to 2016. The results showed that with the improvement in the adaptability of influencing factors, the social vulnerability of Shenzhen continued to decrease [21]. These vulnerability evaluations have mainly focused on smaller scales and neglected the relationship between urban economic development and temporal changes in China's coastal areas. Consequently, in addition to focusing on the temporal and spatial changes in vulnerability, another focus of this study is the relationship between urban economic development and temporal changes in vulnerability in China's coastal areas. This paper analyzes the temporal trends of vulnerability of different types of coastal cities in China from the perspective of human activities with different degrees of impact on coastal cities. Furthermore, this paper explores the internal link between economic development and vulnerability in coastal cities, revealing how the acceleration of economic development and urbanization affects the changes in the vulnerability of coastal areas. At the same time, in order to further discover the patterns of rapid adaptation to extreme events such as storm surge disasters in China's coastal areas, relevant departments should take relevant measures on the basis of the discovered patterns, so as to reduce the impact of storm surge disasters on built-up areas, transportation infrastructure, and other departments in coastal areas.

Aiming to reveal the temporal and spatial changes in the vulnerability of different types of coastal cities in China and the internal relationship between economic development and vulnerability, this paper proposes the following: (1) to analyze the temporal and spatial variation characteristics and differences in the vulnerability intensity of different types of cities in coastal areas from 1990 to 2020; and (2) to explore the relationships between exposure, adaptability, sensitivity and vulnerability, and further reveal the factors that affect the changes in vulnerability. This study provides a scientific basis for disaster prevention and mitigation in China through an in-depth analysis of the temporal and spatial changes in the vulnerability of different types of cities along the coast of China and their internal causes, while providing a research example to reduce the risk of global storm surge disasters.

2. Study Area and Data

2.1. Study Area

At present, increased human activities are increasing the vulnerability of coastal areas to natural disasters such as storm surges [22]. Therefore, we comprehensively selected four types of city to evaluate their vulnerability based on the different degrees of impact of human activities on vulnerability, with different levels of urban development, rapid urban impervious surface expansion, rapid changes in cultivated land area, and high total fishery output value. First of all, considering the level of development of China's coastal urbanization, diverse urbanization process regions have different post-disaster reconstruction and recovery capabilities, resulting in disaster-affected bodies in the face of disasters with unlikely anti-risk capabilities. Secondly, in coastal areas where large-scale coastal facilities—such as industrial and mining plants and entertainment facilities—are concentrated, their manifestation is an impervious surface. Finally, agriculture and fisheries in coastal cities suffer huge economic losses because of the impact of storm surge disasters, and they possess poor economic recovery ability after disasters. After creating a 10 km buffer zone based on the coastline, the impervious surface and cultivated land area in the coastal areas in 1990 and 2020 were calculated, and the impervious surface and cultivated land change rates of different cities in the coastal areas of the country over the past 30 years were calculated. Figure 1a,b show the top 20 cities in terms of impervious surface and cultivated land change rate in China's coastal areas, respectively. The top 20 cities in the country's coastal areas in terms of urban fishery output value in 2020 are shown in Figure 1c.

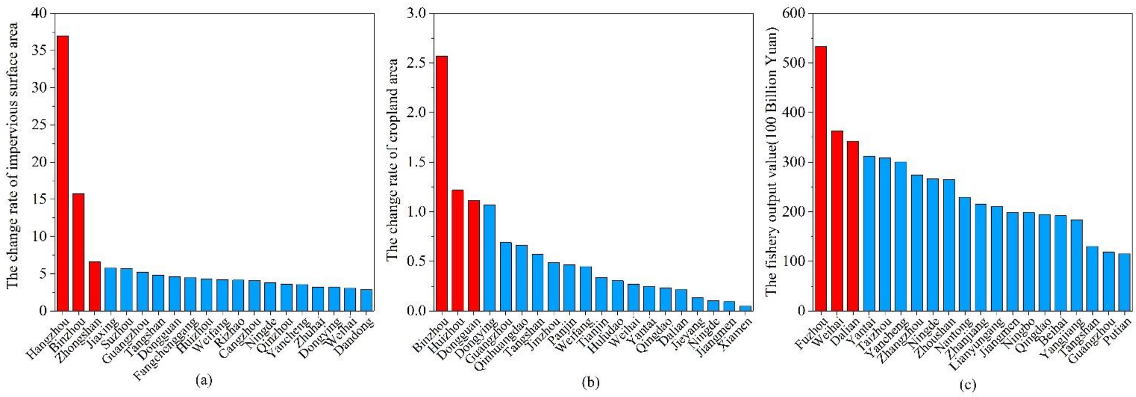

Figure 1. Top 20 rankings of different types of change in cities in China: (**a**) China's coastal cities ranked among the top 20 cities in terms of the change rate of impervious surface area. (**b**) China's coastal cities ranked among the top 20 cities in terms of the change rate of cultivated land area. (**c**) China's coastal cities ranked among the top 20 cities in terms of fishery output value in 2020. The red bars show the top three cities for each indicator.

Combined with the above analysis, we selected representative cities from the following perspectives: (1) Urbanization level—Shanghai, Guangzhou, Shenzhen, Tianjin, Weifang, Yancheng, and Zhanjiang were selected as cities with different levels of urban development. (2) The rate of change of the impervious surface—Figure 1a shows that the impervious surface change rates of Hangzhou, Binzhou, and Zhongshan were 3640%, 1573%, and 658%, respectively. Therefore, Hangzhou and Zhongshan were selected as the urban impervious-surface-expansion-type cities. (3) The rate of change of cultivated land—Figure 1b shows that the change rates of cultivated land in Binzhou, Huizhou, and Dongguan were 257%, 122%, and 111%, respectively. Binzhou, Huizhou, and Dongguan were therefore selected as agricultural-development-type cities. (4) Fishery output value—The fishery output value of Fuzhou, Weihai, and Dalian was CNY 53.31 billion, CNY 36.26 billion, and CNY 34.24 billion, respectively, so the above three cities were selected as fishery-type cities. Figure 2 shows the geographical distribution of the different types of coastal cities in China.

2.2. Data

2.2.1. Land Cover Data

The timespan of this study was 30 years, from 1990 to 2020, so it was necessary to select a land-use dataset that satisfied the time change. We selected the GLC_FCS30-2020 dataset of the latest global 30 m surface coverage fine classification product developed by the team of Mr. Liu Liangyun, from the Institute of Aerospace Information Innovation, Chinese Academy of Sciences, in 2020. The dataset includes 30 m fine surface coverage dynamic monitoring products for the whole year, from 1985 to 2020, including a total of 29 types of land cover, with a 5-year update cycle [23]. The data source link is http://data.casearth.cn/sdo/detail/5fbc7904819aec1ea2dd7061 (accessed on 5 January 2023). The classification of land use is shown in Table A1.

2.2.2. DEM Data

A digital elevation model (DEM) can reflect the absolute terrain and terrain fluctuations in the study area. We adopted NASADEM—a dataset with a spatial resolution of 30 m, which uses an improved algorithm to reprocess the original signal radar data of Shuttle Radar Topography Mission (SRTM) and combines the data from ice, cloud, and land elevation satellites (ICESat). The data from the System for Earth Science Laser Altimeter and the Advanced Spaceborne Thermal Emission and Reflection Radiometer (ASTER) tool were used, which are publicly available on the Google Earth Engine (GEE) platform. NASADEM's data are distributed in 1 degree latitude by 1 degree longitude tiles and consist of all land between 60° N and 56° S latitude. This accounts for about 80% of Earth's total landmass. The data source link is https://lpdaac.usgs.gov/products/nasadem_hgtv001/ (accessed on 5 January 2023).

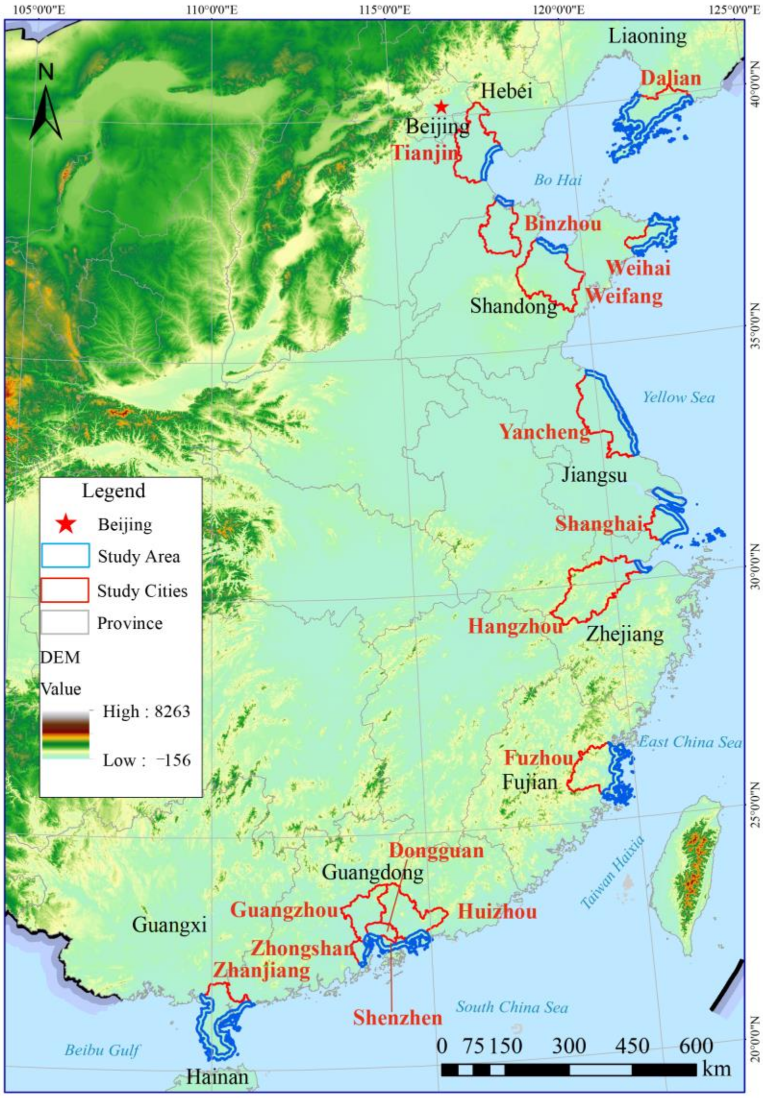

Figure 2. The geographical distribution of different types of coastal cities in China.

2.2.3. Statistical Data of Each City

The seven indicators of adaptive selection were general public budget expenditure (CNY 100 million), gross domestic product (GDP) (CNY 100 million), per capita disposable income of urban residents (CNY), per capita disposable income of rural residents (CNY), investment in fixed assets (CNY 100 million), number of medical technical personnel of hospitals and health centers (persons), and number of hospitals and health centers (number). The sensitivity indicators included four categories, namely, the proportion of females in the total population (%), number of students in enrollment (10,000 people), proportion of primary industry in GDP (%), and proportion of fishery output value in GDP (%). The seven adaptive and four sensitivity indicators resulted in a total of 11 indicator categories. The data sources for each indicator are shown in Table 1.

Table 1. Data sources for adaptive and sensitivity indicators.

	Data Type	Description	Source
B1	General public budget expenditure	Million CNY	China City Statistical Yearbook 1990–2020
B2	GDP	Million CNY	China City Statistical Yearbook 1990–2020
B3	Per capita disposable income of urban residents	CNY	Statistical yearbook data of each city
B4	Per capita disposable income of rural residents	CNY	Statistical yearbook data of each city
B5	Investment in fixed assets	Million CNY	Statistical yearbook data of each city
B6	Number of medical technical personnel of hospitals and health centers	Persons	China City Statistical Yearbook 1990–2020
B7	Number of hospitals and health centers		China City Statistical Yearbook 1990–2020
C1	Proportion of females in the total population	%	Population census data and Statistical yearbook data of each city
C2	Number of students in enrollment	10,000 people	China City Statistical Yearbook 1990–2020
C3	Proportion of primary industry in GDP	%	China City Statistical Yearbook 1990–2020
C4	Proportion of fishery output value in GDP	%	Statistical yearbook data of each city

3. Methods

This study evaluates the vulnerability of coastal cities through the three dimensions of exposure, adaptability, and sensitivity, and finally obtains the overall vulnerability evaluation results of administrative units by calculating and evaluating the weights of each dimension. The comprehensive evaluation process is shown in Figure 3.

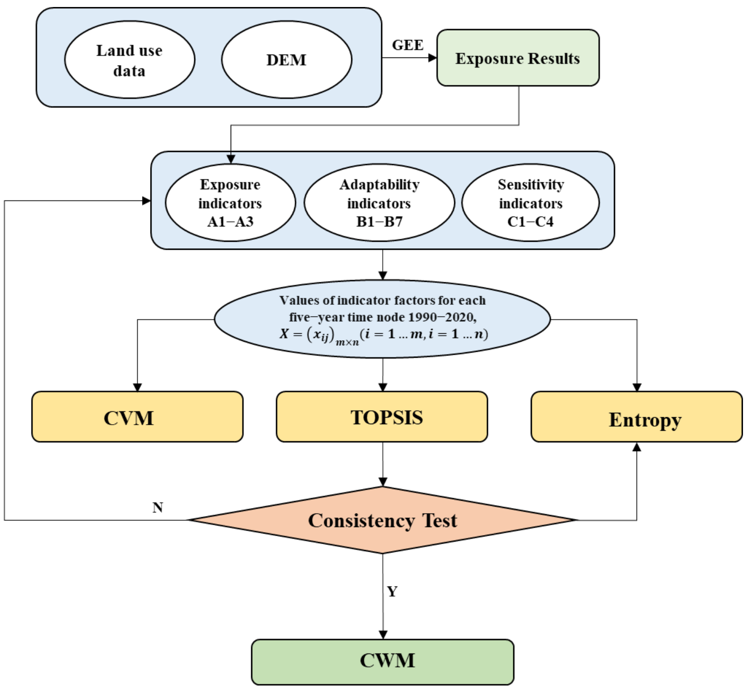

Figure 3. Flowchart of integrated vulnerability assessment methodology.

3.1. Calculation and Change of Exposure

Exposure refers to the background vulnerability of the disaster-bearing body and is one of the important indicators in comprehensive vulnerability evaluations [24]. In this study, a method based on the existing land cover data and the physical characteristics of the disaster-bearing body was used to evaluate the degree of urban exposure. Table 2 illustrates the exposure index factor weight assignment, and the exposure calculation formula is as follows:

$$\text{Exposure} = p1 \times \text{Landcover} + p2 \times \text{Elevation} + p3 \times \text{Slope} + p4 \times \text{Distance to water} \quad (1)$$

Table 2. Exposure index factor weight assignment.

Indicator	Judgement Criterion	Exposure Value	Experts' Score	Weight
Land cover	Impervious surfaces Cropland Wetland Forest Water/bare areas	1 0.8 0.6 0.4 0.2	9	0.5
Elevation	<1 m =1 m >1 m	1 0.6 0.2	3	0.167
Slope	<0.5° 0.5−15° >15°	1 0.6 0.2	2	0.111
Distance to water	≤0.5 km 0.5–1 km 1–2 km 2–5 km >5 km	1 0.8 0.6 0.4 0.2	4	0.222

In this formula, land cover, elevation, slope, and distance to water are the land cover type, elevation, slope, and the distance from the water system, respectively, multiplied by the weights p1, p2, p3, and p4 of each index to obtain the final exposure result value. Among them, each or several types of land cover correspond to a type of disaster-bearing body. According to the characteristics of the intensity of human activity in the land cover types, the 29 types of land cover were divided into five types of disaster-bearing bodies with different properties. These were recast as impervious surfaces, cropland, wetland, forest, and water/bare areas. According to the Technical Guidelines for Storm Surge Disaster Risk Assessment and Zoning issued by China in 2016, which is a normative technical document for storm surge disaster risk assessment and zoning, different vulnerability values are set for different land-use types. Therefore, this paper improves the evaluation index system on the basis of the above guidelines. Taking the vulnerability of each land-use type as the background vulnerability of the disaster-bearing body, this is involved in the comprehensive vulnerability evaluation of the disaster-bearing body. Moreover, exposure is closely related to the physical characteristics of the region and is the natural attribute of the disaster-bearing body. In this study, elevation, slope, and distance from the water system were selected as the physical characteristics of the disaster-bearing body. A low altitude, gentle slope, and shorter distance to the water system indicate that the disaster-bearing body is more sensitive to disasters such as storm surges and, hence, the degree of exposure for the region is higher. The exposure factor weights were determined by the expert scoring method and the multilevel analysis method. In this study, indicators in the expert scoring method were mainly scored by referring to the team's existing research results [25]. The weights of each indicator were assigned as shown in Table 2. The weight results for the above formulae were p1 = 0.5, p2 = 0.167, p3 = 0.111, and p4 = 0.222.

The above calculation process for the exposure index of coastal cities was implemented in GEE. The exposure level in the calculation result was expanded by 10 times and rounded up, and the result value was divided into 2–10 levels. Figure 4 shows a frequency distribution map of the exposure grade area in 15 coastal cities of China from 1990 to 2020. The distribution of exposure grades in Tianjin changed significantly. In 1995, there was a single peak and the area of exposure grade 4 was 420.21 km^2. After 2000, the distribution of exposure grades showed double peaks, and the area values of exposure for grades 4 and

7 of Tianjin in 2000–2020 were 321.04 km^2 and 215.97 km^2, respectively. The distribution of exposure grades in Binzhou has always had a unimodal pattern, changing from grade 6 in 2000 to grade 2 in 2005. Before 2000, the average area of exposure for grade 6 of Binzhou was 230.67 km^2. The average area of exposure for grade 2 of Binzhou from 2000 to 2020 was 263.35 km^2. The seven cities of Shanghai, Yancheng, Zhanjiang, Hangzhou, Dongguan, Weihai, and Dalian showed an obvious concentration peak in terms of the distribution of exposure grades. Shanghai and Zhanjiang showed the highest distribution area of exposure at grade 6, with an average area of 1437.10 km^2 and 2265.36 km^2, respectively. Yancheng, Hangzhou, and Dongguan showed the highest distribution area of exposure at level 7, with an average area of 1116.07 km^2, 190.64 km^2, and 95.51 km^2, respectively. The fishery-type cities, represented by Weihai and Dalian, showed the highest area value of exposure level 4; the areas were 1568.51 km^2 and 3017.77 km^2, respectively. Guangzhou, Shenzhen, Weifang, Zhongshan, Huizhou, and Fuzhou had two distinct peaks in the frequency distribution of exposure grades. The average area difference between the two peaks in Guangzhou was the highest, at 62.52 km^2, and the average area difference between the two peaks in Weifang was the smallest, at 10.64 km^2.

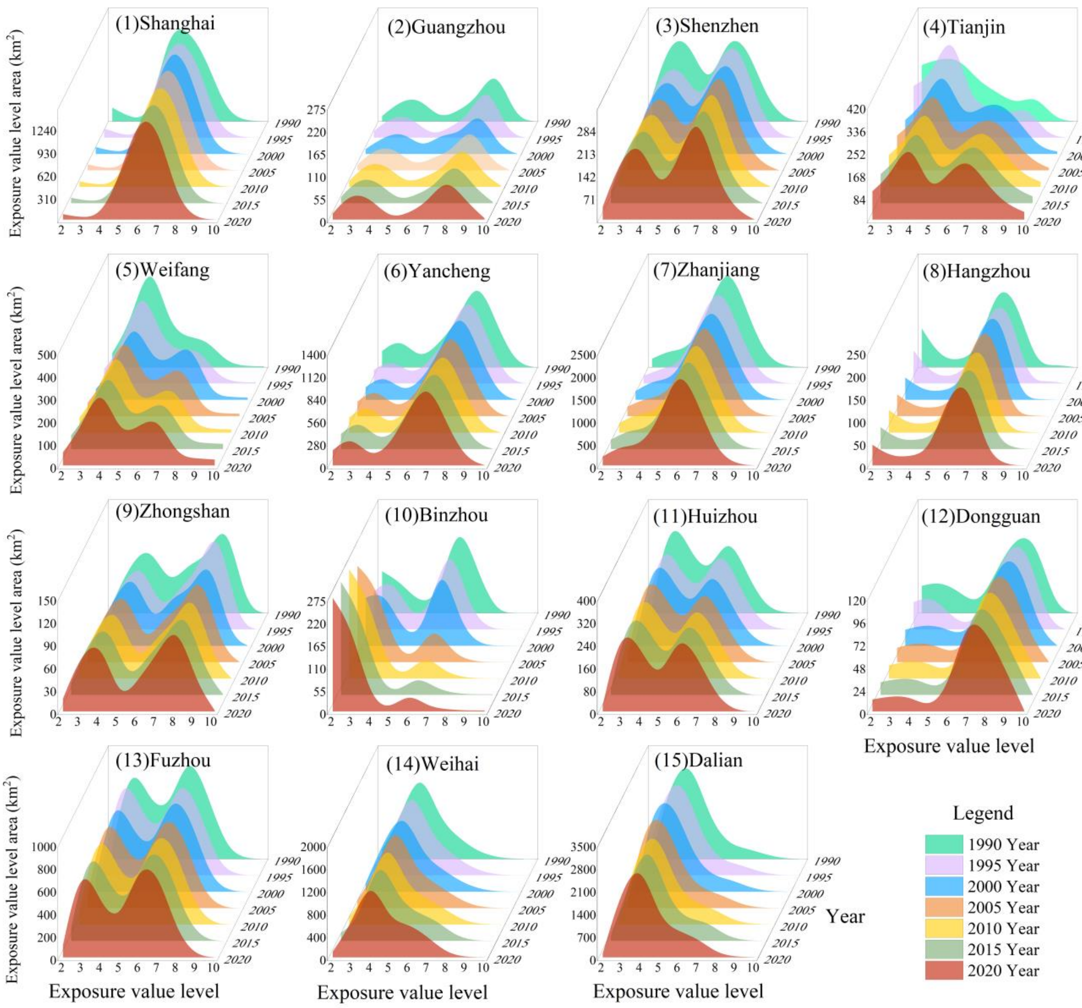

Figure 4. Frequency distribution map of exposure grade area in 15 coastal cities of China from 1990 to 2020.

After 2000, there was no significant inconsistency in the distribution of urban exposure grades in Tianjin and Binzhou, while the changes in exposure grade area in other cities from 1990 to 2020 were consistent with single or double peaks. The above analysis results suggest that the exposure of coastal cities in China has not significantly changed in the past 20 years.

3.2. Change of Sensitivity Indicators

Sensitivity mainly reflects the population and economic losses of cities that are vulnerable to storm surge disasters. An increase in sensitivity will reduce a region's ability to resist risks, enhancing the region's vulnerability [26]. The proportion of females in the total population and the number of students in enrollment were selected considering that the higher the proportion of females and students in the city, the larger the groups affected by disaster in the city. The higher the proportion of primary industry and fishery output value in GDP, the higher the probability of urban poverty rate, the higher the cost of post-disaster recovery, and the lower the resilience.

Figure 5 illustrates the trend chart of sensitivity index values after positive standardization in 15 coastal cities of China, from 1990 to 2020. The aim of positive standardization is to eliminate the influence of dimension and distribution differences on each indicator. The formula for positive standardization is as follows:

$$x'_{ij} = \left(x_{ij} - \mathrm{MIN}\left(x_j\right)\right) / \left(\mathrm{MAX}\left(x_j\right) - \mathrm{MIN}\left(x_j\right)\right) \tag{2}$$

where x_{ij} is the original evaluation index matrix, while MAX and MIN represent the maximum and minimum values of the index value in column j, respectively. From 1990 to 2020, the proportion of primary industry in GDP and the proportion of fishery output value in GDP in the sensitivity indicators showed a continuous downward trend, the number of students in enrollment in other cities except for Yancheng continued to increase, and the proportion of females in the total population in each city showed no obvious trend. Table A2 shows the annual mean change rates for the sensitivity indicators in the 15 coastal cities from 1990 to 2020 and further analyzes the changes in the sensitivity indicators in those 15 coastal cities. From 1990 to 2020, the average growth rate of the proportions of primary industry and fishery output value in GDP in the 15 coastal cities was negative. The proportion of primary industry in GDP in Yancheng and Weihai declined the fastest on average, with an average decline rate of 0.012%/year and 0.011%/year, respectively. As of 2020, the proportion of primary industry in GDP in Yancheng and Weihai was 11.10% and 10.01%, respectively. The proportion of fishery output value in GDP in Weihai declined the fastest on average, with an average decline rate of 0.007%/year. In 1990 and 2020, the proportion of fishery output value in GDP in Weihai City was 0.32% and 0.12%, respectively. From 1990 to 2015, the average rate of decline in the number of students in enrollment in Yancheng City was 0.7626 ten thousand people/year, the number of students enrolled in school in 1990 was 1,148 thousand, and the number of students enrolled in school in 2015 was 788.8 thousand. The annual number of students in school was positive, with an average annual growth rate of 2.61 ten thousand people/year during 2015–2020. As of 2020, the number of students in enrollment in Yancheng was 919.2 thousand. The number of students in enrollment in Guangzhou and Shenzhen showed the largest annual growth rate, with an average growth rate of 7.08 ten thousand people/year and 5.28 ten thousand people/year, respectively. In 2020, the number of students enrolled in Guangzhou and Shenzhen was 3.10 million and 1.79 million people, respectively. From 1990 to 2020, the regularity of the proportion of females in the total population was not obvious. The average growth rate of the proportion of females in the total population in Tianjin, Yancheng, Zhanjiang, Fuzhou, and Dalian was greater than 0, while the average growth rate of the proportion of females in the total population in Weifang, Binzhou, and Weihai was equal to 0, and the average growth rate of the proportion of women in the other cities was less than 0.

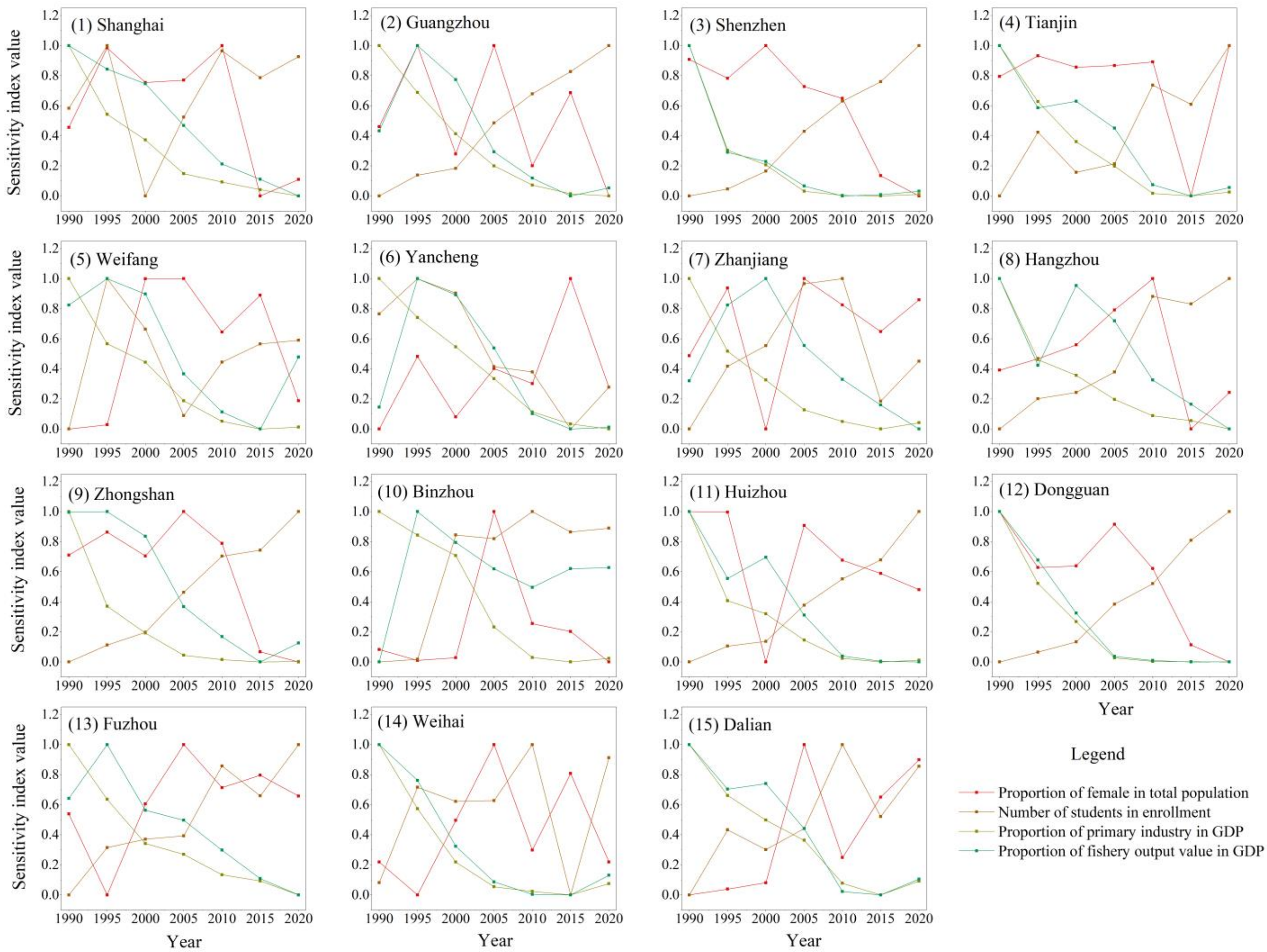

Figure 5. Trend chart of sensitivity index values after positive standardization in 15 coastal cities of China from 1990 to 2020.

3.3. Change of Adaptability Indicators

Adaptability mainly reflects coastal cities' ability to respond to disasters, and adaptability is crucial to alleviating urban vulnerability [27]. This article's adaptability research looks at three perspectives: social resistance, social resilience, and social self-healing. Selecting general public budget expenditure, GDP, and investment in fixed assets as aspects of social resistance indicates that the higher the economic development and infrastructure investment of cities in the region, the stronger the cities' ability to resist social risks in the face of disasters. The per capita disposable income of urban residents and the per capita disposable income of rural residents are the determinants of social resilience; the higher the resilience, the stronger the residents' economic adjustment ability in the face of disaster. The number of medical technical personnel in hospitals and health centers, along with the number of hospitals and health centers, represent the social self-healing capabilities; the higher the proportion, the richer the urban medical resources and the stronger the self-healing ability [21,25].

Figure 6 illustrates the change trend chart of adaptability index values after negative standardization in 15 coastal cities of China from 1990 to 2020. The actual situation of the adaptive index of each coastal city in China is changing with time, and the result value is continuously increasing. Table A3 shows the annual mean change rate of the adaptability index in 15 coastal cities from 1990 to 2020. To be consistent with the positive and negative relationships between the vulnerability results in this paper, we negatively normalized the adaptive index, and the negative normalization formula is as shown in Equation (3). The maximum value in the adaptive index is normalized to the minimum value, so the standardized results of each adaptive index in Figure 6 continue to decrease with time.

$$x'_{ij} = (\mathrm{MAX}(x_j) - x_{ij}) / (\mathrm{MAX}(x_j) - \mathrm{MIN}(x_j)) \quad (3)$$

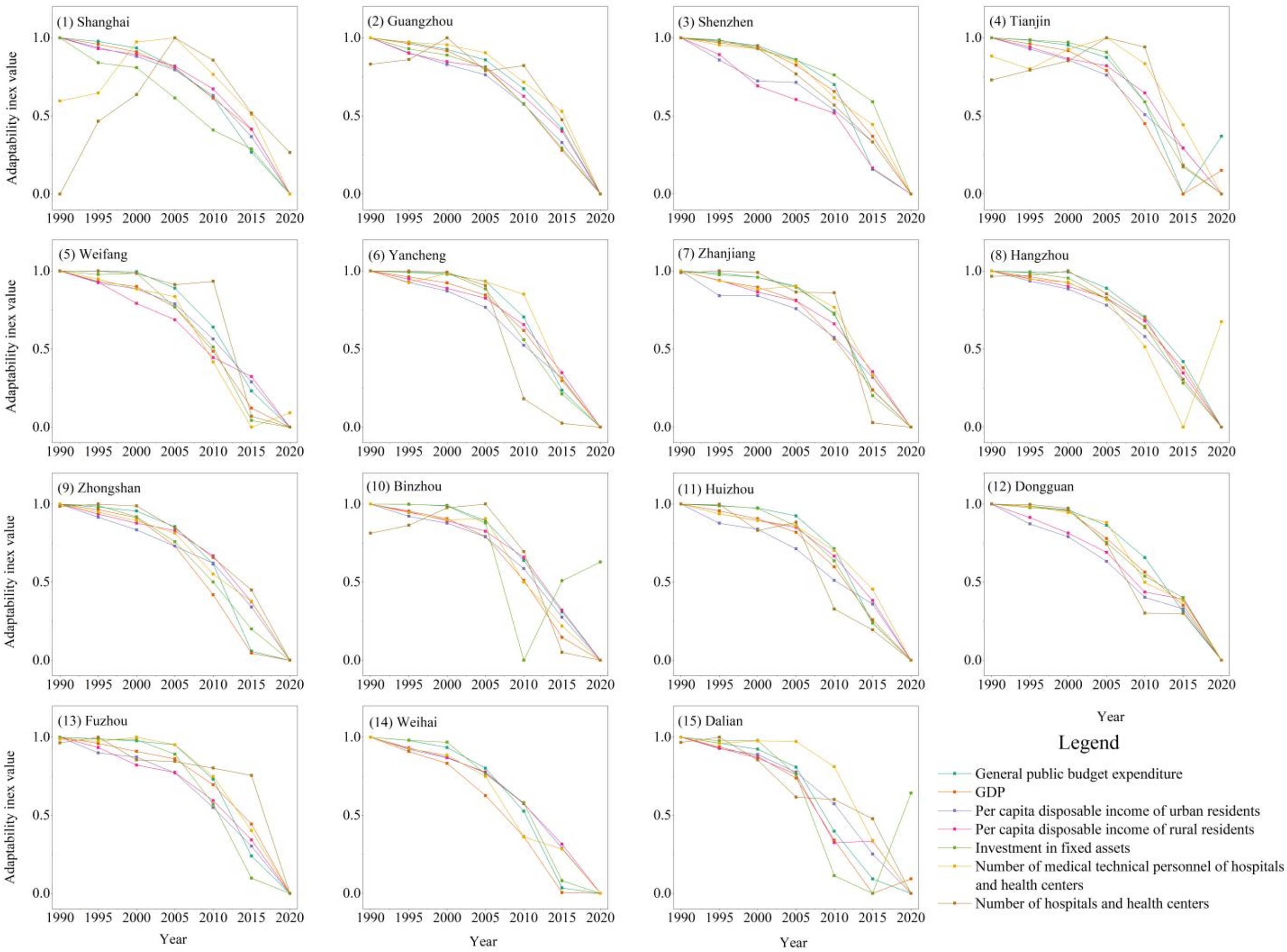

Figure 6. The change trend chart of adaptability index values after negative standardization in 15 coastal cities of China from 1990 to 2020 (the smaller the value, the stronger the adaptability).

From 1990 to 2020, there was an obvious turning point in the number of medical technical personnel of hospitals and health centers, as well as in the number of hospitals and health centers, in Shanghai in 2005. The number of medical technical personnel at hospitals and health centers in Hangzhou dropped sharply in 2020. The investment in fixed assets in Binzhou and Dalian reached their highest values in 2010 and 2015, respectively. The results of the urban adaptation indicators show a continuous downward trend.

Table A3 shows the average annual change rate of each city's adaptability indicators over the past 30 years and further analyzes the changes in those adaptability indicators. In 1990, the number of medical technical personnel in hospitals and health centers and the number of hospitals and health centers in Shanghai were 158.50 thousand people and 7690, respectively. In 2005, the number of medical technical personnel in hospitals and health centers and the number of hospitals and health centers were 103.5 thousand people and 2527, respectively. From 1990 to 2005, the number of medical technical personnel in hospitals and health centers and the number of hospitals and health centers in Shanghai continued to decrease; the average annual decline rates were 3.7 thousand people/year and 344/year, respectively. The number of medical technical personnel in hospitals and health centers and the number of hospitals and health centers in Shanghai increased from 2005 to 2020, and the annual average added values were 9073.3 thousand people/year and 253/year, respectively. As of 2020, the number of medical technical personnel in hospitals and health centers and the number of hospitals and health centers in Shanghai were 2396 thousand people and 6317, respectively. The number of medical technical personnel in hospitals and health centers in Hangzhou in 2015 was 93.04 thousand people and, as of 2020, 51.14 thousand people, showing that the number of medical technical personnel in hospitals and health centers significantly decreased. The average annual growth rate of the number of medical technical personnel in hospitals and health centers in Guangzhou was the highest, with a value of 5.54 thousand people per year. In 2020, the number of medical technical personnel in hospitals and health centers in Guangzhou was 214.61 thousand people. The number of hospitals and health centers in Weifang was the largest in 2020, with a value of 8150. The average annual growth rate of the number of hospitals and health centers in Weifang was 238 per year.

The cities of Shanghai, Shenzhen, and Guangzhou were developing rapidly, and the cities accumulated a lot of wealth. The general public budget expenditure and GDP of these three cities were relatively high. In 2020, the general public budget expenditures of the three cities of Shanghai, Shenzhen, and Guangzhou were CNY 843.086 billion, CNY 417.842 billion, and CNY 295.265 billion, respectively, with an average annual growth rate of CNY 27.851 billion/year, CNY 13.862 billion/year, and CNY 9.761 billion/year, respectively. Their GDP was CNY 4321.485 billion, CNY 2767.024 billion, and CNY 2501.911 billion, respectively, and their average annual growth rates were 141.567 billion CNY/year, 91.781 billion CNY/year, and 82.332 billion CNY/year. In 1990, Tianjin's investment in fixed assets was CNY 7.208 billion. As of 2020, Tianjin's investment in fixed assets was CNY 1,575.955 billion. The annual growth rate of Tianjin's investment in fixed assets was CNY 52.292 billion per year. Tianjin's investment in fixed assets in 2020 was 1.78 times that of the second highest city (Shanghai). The investment in fixed assets in Binzhou reached its highest value of CNY 404.789 billion in 2010, and it was CNY 150.118 billion as of 2020. Its rule for investment in fixed assets was to first increase and then decrease, with an average growth rate of CNY 4.996 billion per year.

As of 2020, the per capita disposable income of urban residents in the coastal areas of Shanghai, Guangzhou, Hangzhou, and Shenzhen was high, at CNY 82,429, CNY 68,304, CNY 68,666, and CNY 64,877.7, respectively, with an average annual growth rate of CNY 2,674.91/year, CNY 2,185.17/year, CNY 2222.70/year, and CNY 2025.02/year, respectively. The urban per capita disposable income of Zhanjiang and Binzhou was low, with an average annual growth rate of CNY 1022.59/year and CNY 1234.00/year, respectively. The average annual growth rates of the per capita disposable incomes of rural residents in the three cities of Hangzhou, Dongguan, and Shanghai were CNY 1250.97/year, CNY 1242.83/year, and CNY 1228.53/year, respectively.

3.4. Comprehensive Weight Assignment Method of Vulnerability

Exposure, sensitivity, and adaptability were combined with three evaluation methods—the entropy weight method ($Entropy$), the coefficient of variation method (CVW), and the $TOPSIS$ method—and the final vulnerability result value W_s was obtained.

$$W_s = CWM(Entropy, CVW, TOPSIS) \tag{4}$$

Among them, entropy in the entropy weight method is a measure of the uncertainty of information. The larger the amount of information, the smaller the uncertainty and the smaller the entropy value. The entropy value is used to measure the discrete degree of decision-making attributes. The greater the discrete degree, the greater the impact on the comprehensive evaluation; therefore, a larger weight should be given [25,28]. The coefficient of variation method means that the attribute with the greater difference in attribute value has a greater influence on the order of the decision-making scheme. To eliminate the influence of different dimensions, the coefficient of variation of attributes was used to measure the degree of difference for each attribute [29]. TOPSIS calculates the weighted Euclidean distance between a certain scheme and the positive ideal solution and the negative ideal solution, determining the closeness of the scheme to the ideal solution to judge the pros and cons of each decision-making scheme [21,30]. The TOPSIS method needs to combine the entropy weight method to determine the indicator weight value and then sort the results of multiple indicators.

3.4.1. Kendall Consistency Test

Since different methods have their own limitations, the conclusions drawn by different models are not the same. However, as long as the evaluation criteria are consistent, the obtained grading results are reasonable. The Kendall consistency test can be used to test whether the evaluation criteria of each model are consistent [31].

$$W = \sum_{i}^{n} \left(R_i - m(n+1)/2\right)^2 / m^2 n \left(n^2 - 1\right)/12 \tag{5}$$

where m is the number of model species, n is the number of samples participating in the evaluation, and R_i is the sum of the ranks of the *i*th sample. The numerator in the formula is the sum of the squares of the deviation of the total rank of each group of samples and the total rank of the whole, while the denominator is the square of the total deviation of the whole rank. Here, m represents three evaluation methods, namely, the entropy weight method, variation coefficient method, and entropy weight–TOPSIS method. When W is closer to 1, this indicates that the rank has a greater difference between groups, which means that there are significant differences in the vulnerability scores obtained for the urban samples participating in the assessment, and further indicates that the assessment standards of different methods are consistent; conversely, if W is greater close to 0, there is no reason to think that the criteria for these methods are consistent.

3.4.2. Combination Weighting Method

At present, there are many methods that can be used to calculate the weights of the evaluation indicators [1]. Due to the different basic principles of the different methods and the different emphases used to determine the weights, the weights of the evaluation indicators obtained by the different methods are inconsistent, and the evaluation conclusions are different. Therefore, the idea of a "combined evaluation" is proposed. Combination weighting is a kind of combination evaluation. The "combination weight" and "combination evaluation value" obtained by combining the results calculated by different methods can improve the reliability and accuracy of the comprehensive evaluation results [32]. The calculation process of the weight combination based on CWM is as follows:

Combined weight coefficients for a single evaluation method:

$$\theta_j^* = \sum_{i=1}^{m} \sum_{t=1}^{m} \left|f_{ij} - f_{tj}\right| / \sum_{j=1}^{n} \sum_{i=1}^{m} \sum_{t=1}^{m} \left|f_{ij} - f_{tj}\right| \tag{6}$$

where f_{ij} and f_{tj} are the evaluation values of i and t, respectively, using the single evaluation method j.

Calculate the combined weights of indicators ω_s:

$$\omega_s = \theta_1^* \overline{\varpi}_{1s} + \theta_2^* \overline{\varpi}_{2s} + \ldots + \theta_n^* \overline{\varpi}_{ns} \tag{7}$$

$\overline{\varpi}_{js}$ is the weight value of each vulnerability index s using method j, where s = 3.

3.5. Result of Consistency Test

The vulnerability assessment of the 15 coastal cities was carried out with the help of three comprehensive evaluation methods: the entropy weight method, the coefficient of variation method, and TOPSIS. Table 3 shows the results of the Kendall's W analysis. The significance value of the vulnerability results of the three comprehensive evaluation methods—the entropy weight method, the coefficient of variation method, and TOPSIS—was 0.000, which is significant at the required level to reject the null hypothesis, so the vulnerability results show consistency. At the same time, the Kendall's W value of the model is 0.214, so the degree of correlation is consistent. Through the Kendall consistency test, it can be proven that the above three comprehensive evaluation methods can use the combination of CWM weights to obtain the final evaluation results.

Table 3. The results of Kendall's W.

Name	Mean Rank	Median	Kendall's W	X^2	p
Entropy	1.971	0.495	0.214	44.933	0.000 ***
CVW	2.476	0.678			
TOPSIS	1.552	0.426			

*** means the result at 1% significance level.

4. Results

4.1. Identifying Storm Surge Vulnerability Distribution Changes

The high areas of vulnerability shifted from the southern region to the northern region. Figure 7 shows the spatial distribution of vulnerability in 15 coastal cities in China from 1990 to 2020. From 1990 to 2020, the vulnerability of the 15 coastal cities decreased. In 1990, the vulnerability of southern cities was higher than that of northern cities. As of 2020, there has been a significant improvement in the vulnerability of southern cities, and their vulnerability is now generally lower than that in northern cities. In 1990, the vulnerability of the 15 coastal cities was relatively high: the vulnerabilities of the southern cities Shanghai, Hangzhou, Fuzhou, Guangzhou, Dongguan, Shenzhen, Huizhou, Zhongshan, and Zhanjiang were all between 0.73 and 0.85. In 2020, the vulnerabilities of the 15 coastal cities were all between 0.13 and 0.43, and the vulnerabilities of Yancheng, Shanghai, Fuzhou, Guangzhou, Dongguan, Shenzhen, Huizhou, Zhongshan, and Zhanjiang were lower than those of the southern cities, with a vulnerability of 0.13–0.23. Only Weifang and Weihai among the northern cities had vulnerability between 0.13 and 0.23.

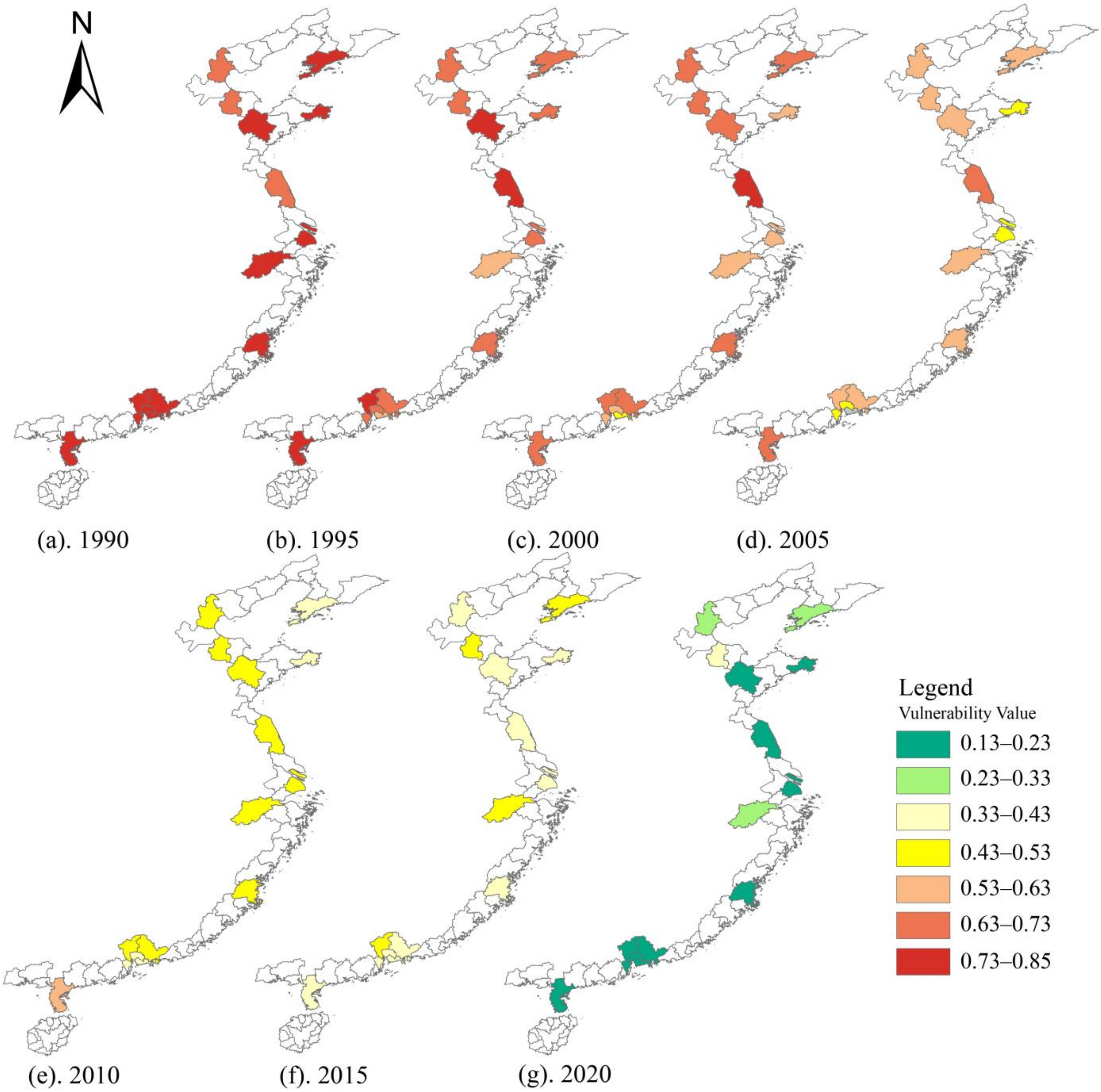

Figure 7. Spatial distribution of vulnerability in 15 coastal cities in China from 1990 to 2020.

4.2. Identifying Coastal Vulnerability Tendencies

From 1990 to 2020, the vulnerability of different types of coastal city in China showed a continuous downward trend, and the average reduction rate for vulnerability in the 10 years from 2005 to 2015 was the highest, at 2.23%.

Figure 8 shows the bar distribution of the mean change velocity of urban vulnerability values from 1990 to 2020. By comparing the median value of the average change speed of the vulnerability in each time period, the average change speed of the vulnerability in the 2010–2015 period was found to be the highest, at a value of −2.40%, followed by the 2005–2010 period, with a value of −2.20%, and the 1995–2000 period, with the lowest average change rate of vulnerability, at a value of −1.00%. Table A4 shows the vulnerability results and the change rate of each stage in the 15 coastal cities from 1990 to 2020. In 1990, Shanghai and Shenzhen, with high levels of urbanization, and Dongguan, with a high level of agricultural development, had higher vulnerability values of 0.80, 0.84, and 0.85, respectively. The agricultural cities of Binzhou, Tianjin, and Yancheng, with medium levels of urbanization, had lower vulnerabilities of 0.64, 0.70, and 0.71, respectively. As of 2020, the vulnerabilities of Shanghai, Dongguan, and Shenzhen were relatively low compared to other cities, at 0.14, 0.16, and 0.19, respectively. The vulnerabilities of Binzhou and Tianjin were higher, at 0.33 and 0.28, respectively. Over the past 30 years, the vulnerability results of Shanghai, Dongguan, and Shenzhen significantly decreased. The change rate of each stage from 1990 to 2020 was less than 0. The vulnerability of Binzhou and Tianjin first increased and then decreased. According to Figure 8, the vulnerability change rate of Binzhou in 1990–2000 was 0.39% and 0.90%, respectively, and the change rate in 2000–2020 was less than 0. Tianjin's vulnerability change rate was 0.10% in 1990–1995. The change rate of vulnerability was less than 0 during 1995–2000 in Tianjin. In 1990 and 2020, the vulnerability value of Yancheng was low, with values of 0.71 and 0.14, respectively. However, the change rate of the vulnerability value in Yancheng from 1990 to 2000 was greater than 0, and the average change rate was 1.88% and 0.19%, respectively. The rate of change in the vulnerability of Yancheng from 2000 to 2020 was less than 0, followed by −3.41%, −3.6%, −4.32%, and −1.92%. The average change rates of the vulnerability results of the impervious-surface-development-type and fishery-type development cities were less than 0, and their vulnerability was continuously decreasing.

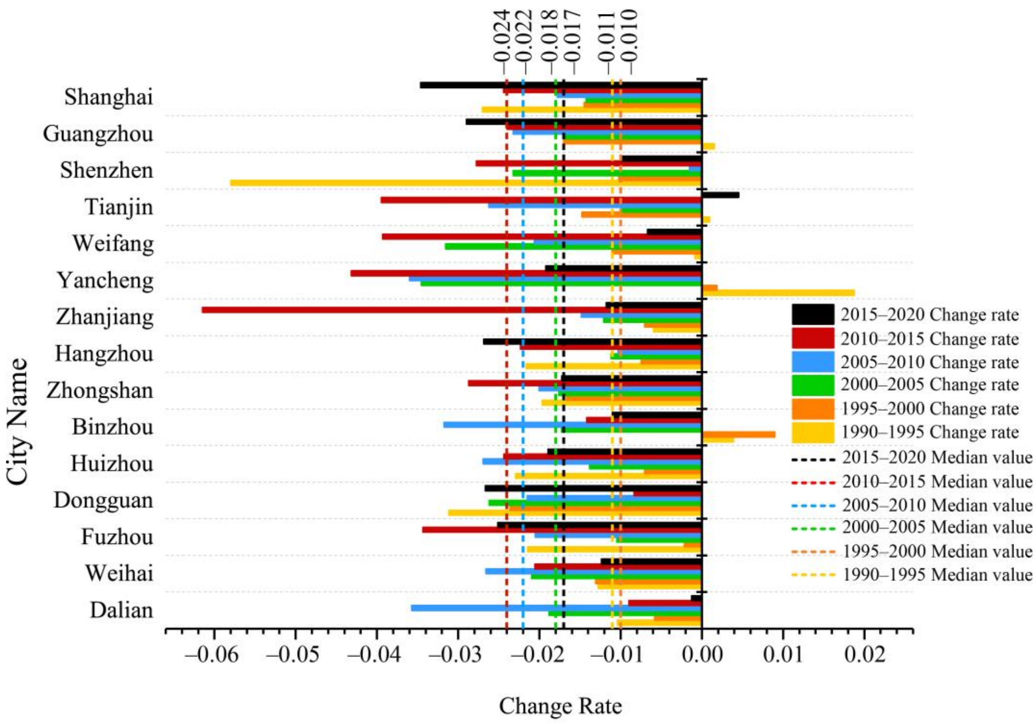

Figure 8. Bar distribution of mean change velocity of urban vulnerability values from 1990 to 2020.

In sum, the urban vulnerability of Shanghai, Shenzhen, and Dongguan changed from relatively high values in 1990 to relatively low values in 2020, the average rate of change in vulnerability over the last 30 years was less than 0, and the urban vulnerability continued to decrease. The vulnerability of Yancheng was relatively low, and its urban vulnerability value first increased and then decreased over time. The vulnerability of Binzhou and Tianjin changed from relatively low values in 1990 to relatively high values in 2020. The average change rate of vulnerability in other cities from 1990 to 2020 was less than 0, indicating that the vulnerability of each city decreased each year in the past 30 years. The above results show that the 15 cities along the coast of China have enhanced their ability to resist risks in the face of natural disasters such as storm surges.

4.3. Adaptability has a Significant impact on Vulnerability

The change law of the vulnerability of each city is greatly affected by the adaptability index, with an average weight of 0.50, while the average weight of the exposure and sensitivity indices is only 0.19 and 0.31, respectively. After the Pearson's correlation test, adaptability and vulnerability were highly positively correlated, so the development trend of vulnerability and adaptability is closely related. Among the adaptability indicators, the general public budget expenditure, investment in fixed assets, GDP, and the level of medical and health services have a greater impact.

Figure 9 shows the temporal changes in vulnerability, exposure, sensitivity, and adaptability in the 15 cities from 1990 to 2020. In the results, the negative standardization of adaptability indicators aims to be consistent with the direction of changes in vulnerability indicators. The change law of the exposure index is not significant. The sum of the sensitivity index values of each city from 1990 to 2000 is 8.16, which is higher than that of 5.01 from 2005 to 2020. The adaptability index in the figure shows a decreasing trend with time. In Table 4, regarding the exposure, adaptability, and sensitivity index weights, cities other than Shenzhen have the highest proportion of adaptability index weights, with an average weight value of 0.47. Therefore, the change law of the vulnerability of each city is greatly affected by the adaptability index. Pearson's correlation test is used to analyze whether there is a significant trend relationship between a set of continuous variables. Therefore, we conducted a Pearson's correlation test to show the vulnerability and the exposure, adaptability, and sensitivity. The results show that only the adaptability indicators pass the correlation test. Changes in vulnerability in cities have the greatest impact.

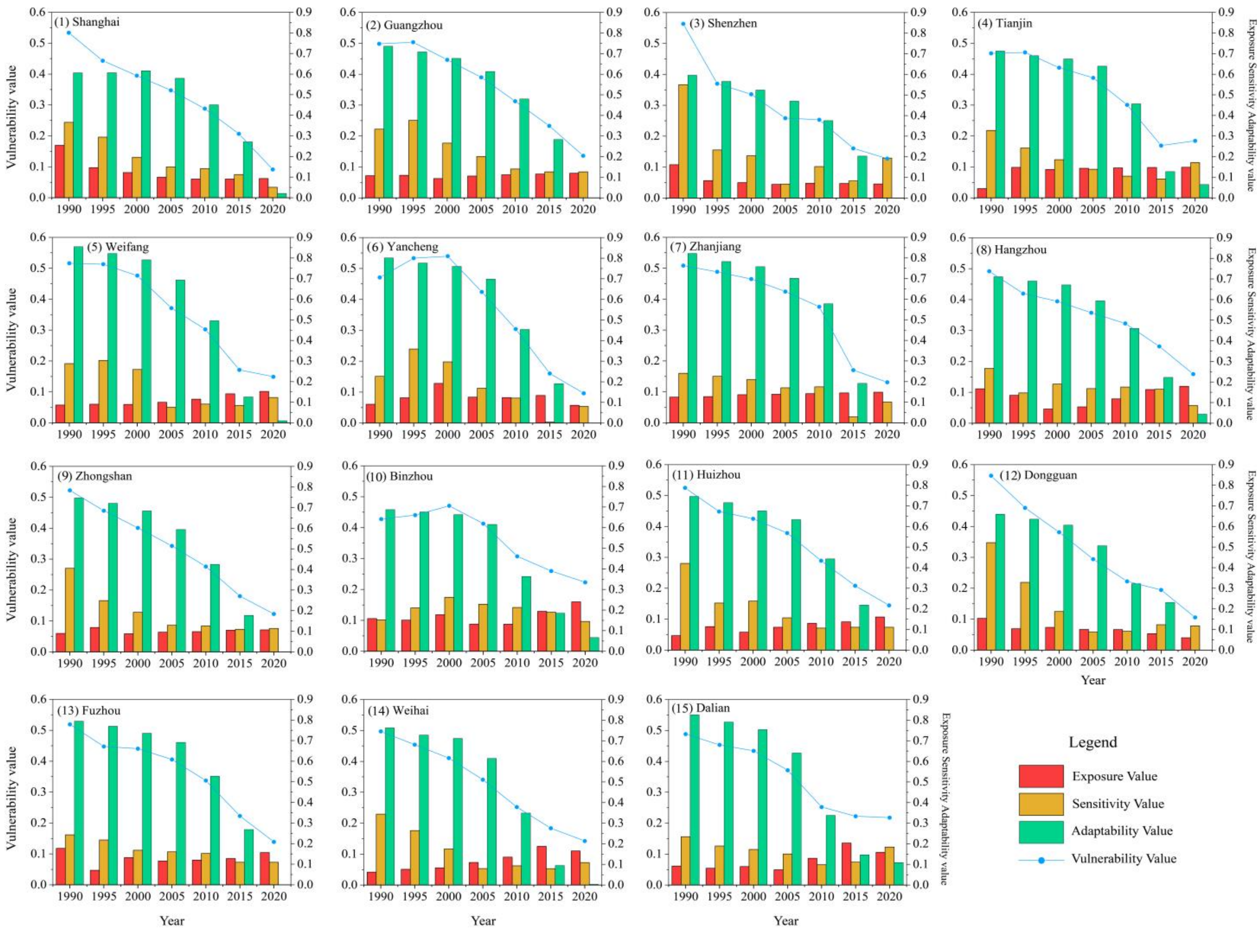

Figure 9. Temporal changes in vulnerability values and internal influencing factors (i.e., exposure, sensitivity, and adaptability) in 15 coastal cities from 1990 to 2020.

Table 4. Exposure, adaptability, and sensitivity index weights and vulnerability correlation values of 15 coastal cities.

City Name	CWM Weight Value			Pearson's Correlation Coefficient		
	Exposure	**Adaptability**	**Sensitivity**	**Exposure**	**Adaptability**	**Sensitivity**
Shanghai	0.25	0.47	0.28	0.78 *	0.92 **	0.95 **
Guangzhou	0.14	0.50	0.36	−0.71	0.98 **	0.91 **
Shenzhen	0.17	0.40	0.44	0.87 *	0.85 *	0.85 *
Tianjin	0.18	0.49	0.32	−0.47	0.98 **	0.71
Weifang	0.17	0.57	0.26	−0.98 **	0.98 **	0.82 *
Fuzhou	0.23	0.53	0.24	−0.13	0.98 **	0.91 **
Hangzhou	0.25	0.48	0.27	−0.34	0.97 **	0.82 *
Zhongshan	0.16	0.50	0.34	−0.29	0.97 **	0.85 *
Binzhou	0.27	0.47	0.26	−0.59	0.98 **	0.57
Huizhou	0.15	0.50	0.35	−0.94 **	0.97 **	0.85 *
Dongguan	0.14	0.44	0.43	0.91 **	0.93 **	0.88 **
Weihai	0.17	0.52	0.32	−0.97 **	0.97 **	0.83 *
Dalian	0.18	0.55	0.27	−0.84*	0.98 **	0.71
Zhanjiang	0.19	0.55	0.26	−0.88 **	0.99 **	0.93 **
Yancheng	0.19	0.53	0.28	0.44	0.98 **	0.91 **

*, ** mean the result at 10% and 5% significance level respectively.

According to the above results, we conducted Pearson's correlation tests between the vulnerability results and the adaptability indicators. Table A5 shows the weight values and vulnerability correlation values of the adaptability index of the 15 coastal cities. The number of medical technical personnel in hospitals and health centers and the number of hospitals and health centers in Shanghai are not highly correlated with changes in urban vulnerability. The reason for this is related to the continuous decreases in the number of medical technical personnel at hospitals and health centers and the number of hospitals and health centers in Shanghai from 1990 to 2005, as well as the continuous increase after 2005 shown in the adaptability index analysis in this article. The number of medical technical personnel at hospitals and health centers in Hangzhou dropped sharply from 2015 to 2020, so the number of medical technical personnel in hospitals and health centers in Hangzhou failed the correlation test. From 1990 to 2020, the investment in fixed assets in Binzhou first increased and then decreased, which was inconsistent with the change trend of vulnerability and, thus, also failed the correlation test. According to the results of the weights of the adaptive indicators of the 15 coastal cities, the weights of the general public budget expenditure, GDP, and investment in fixed assets in the adaptability indicators of Guangzhou, Shenzhen, Tianjin, Fuzhou, Hangzhou, Zhongshan, Binzhou, Huizhou, and Dalian were more than high. The average weights were 0.08, 0.06, 0.09, 0.09, 0.08, 0.09, 0.07, 0.08, and 0.10. For Weifang, Dongguan, Weihai, Zhanjiang, and Yancheng, has the high value of the number of hospitals. Only in Shanghai's adaptability indicators were the weights of general public budget expenditure, GDP, and per capita disposable income of urban residents relatively high.

In sum, the effective adjustment of disaster prevention and mitigation in coastal cities over the past 30 years can be improved by improving urban adaptability. Continuously increasing the general public budget expenditure, investment in fixed assets, and GDP can effectively alleviate storm surge disasters in the region. The higher the adaptability index of the city, the lower the city's vulnerability. Similarly, by improving the medical standards and health of the city, the regional disaster prevention and mitigation capacity can be effectively strengthened. From 1990 to 2020, the exposure of the cities did not significantly change; the sensitivity index values only significantly changed from 1990 to 2000, and then there was only a small fluctuation over the next 20 years. Therefore, the cities can reduce their exposure and sensitivity to improve urban vulnerability. However, relevant departments can control the growth rates of exposure and sensitivity to alleviate the vulnerability of cities in the face of storm surge disasters and effectively improve their urban disaster prevention and mitigation capabilities.

5. Discussions

5.1. Significance of Spatiotemporal Variations in Vulnerability

This paper conducted an in-depth analysis of the changes in the vulnerability of 15 cities along the coast of China during the period from 1990 to 2020, revealing the temporal and spatial changes in the resilience of coastal areas in China in the face of storm surge disasters. The results show that China had the highest average rate of change in vulnerability from 2005 to 2015, and we summarized the frequency of storm surges in China's coastal areas over the 20 years from 2000 to 2021 (Figure 10a). The period of most frequent occurrence of storm surge disasters and the period of highest direct economic losses in China were both from 2005 to 2013. The above data show that the change patterns of vulnerability in China, with high values, are consistent with the period of frequent storm surge disasters in China. The frequency of storm surges and the distribution of direct economic losses in various coastal areas were determined (Figure 10b,c) and compared with the change laws of vulnerability in each city (Figure 8). The frequency of disasters and the direct economic losses in Guangdong in the past 20 years were the highest, at 18.44% and CNY 69.827 billion, respectively. Among the dynamic results of vulnerability, Guangdong's representative cities—Guangzhou, Shenzhen, Zhanjiang, Zhongshan, Huizhou, and Dongguan—were vulnerable in 1990 and 2020. The annual median values were 0.79 and 0.19, respectively, and the range of change was −75.30%, which confirmed that the spatial distribution of the high-value vulnerability changes was consistent with the areas with high levels of disaster frequency, both in Guangdong. In Section 4.3, the analysis of the reasons for the changes in vulnerability shows that adaptability has the highest weight with respect to urban vulnerability. The Pearson's correlation results confirm that general public budget expenditure, GDP, investment in fixed assets, and medical care are related to the changes in vulnerability in the adaptability indicators. Especially in the Guangdong region, where storm surge disasters are frequent and direct economic losses are too high, this proves that improving adaptability can effectively alleviate the vulnerability of cities in the face of storm surge disasters. Therefore, this article shows that, due to the frequent storm surge disasters in the city over a certain period of time, the government strengthened the input of relevant resources in the adaptability index, which ultimately led to the city's vulnerability decreasing more quickly in this period of time.

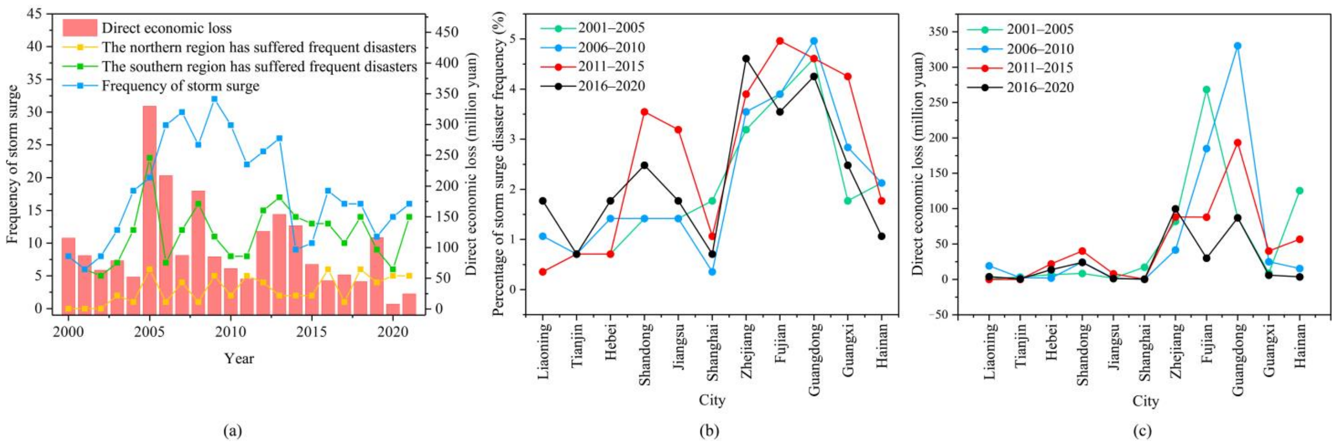

Figure 10. (**a**) Frequency of occurrence of storm surge disasters in China's coastal areas, disaster frequency in southern and northern regions (dot plot), and direct economic losses from storm surge disasters (bar chart) from 2000 to 2021. (**b**) Storm surge disaster frequency as a percentage of total disaster frequency in coastal areas of China from 2001 to 2020. (**c**) Direct economic losses from storm surge disasters in coastal areas of China from 2001 to 2020.

In conclusion, from the perspective of adaptability, we analyzed the temporal and spatial variation characteristics of the vulnerability of coastal areas to discover the change law of the anti-risk capability of coastal areas in China. Continuously improving the social, economic, and adaptability capacity of coastal cities in the face of storm surge disasters is one of the effective measures to reduce the vulnerability of coastal areas facing storm surge disasters.

5.2. Adaptability Enhancement Effect

Globally, China is one of the countries most frequently and severely affected by storm surge disasters. From 2000 to 2020, storm surges occurred 397 times in China, resulting in direct economic losses of up to CNY 220.64 billion [33]. The main purpose of this paper was to evaluate the temporal and spatial changes in coastal vulnerability to determine how coastal areas can quickly adapt to extreme events such as storm surge disasters and reduce the direct economic losses that storm surge disasters cause in various sectors, such as buildings and transportation infrastructure, in coastal areas. Many experts and scholars have analyzed the vulnerability of coastal areas in the face of storm surge disasters from different angles. Many factors affect the vulnerability of coastal areas. First, coastal areas suffer from a high frequency of disasters, resulting in serious property losses and casualties in coastal areas [14,34]. Second, high levels of social sensitivity—such as population aggregation, economic development, unbalanced population structure, and educational attainment—lead to high regional vulnerability [35–37]. Third, factors such as low-lying coastal areas, flat terrain, and physical structures without topographic barriers lead to high regional vulnerability [11,38]. This study mainly evaluated the change characteristics of the vulnerability of 15 typical cities along the coast of China. According to the spatial distribution results, the vulnerability results of cities in southern China in 2020 are lower than those in northern cities, among which Shanghai, Shenzhen, and Dongguan have the lowest vulnerability. In terms of time change, urban vulnerability continued to decline from 1990 to 2020. Compared with exposure and sensitivity, adaptability contributed more to the decline in urban vulnerability. Therefore, the temporal and spatial changes in vulnerability in this paper are closely related to the changes in the factors affecting coastal vulnerability, indicating that it is feasible and effective to reduce vulnerability by improving the adaptability indicators of factors affecting vulnerability. Furthermore, existing research indicates that, in order to take necessary measures to alleviate the vulnerability of coastal areas, in addition to the necessary coastal engineering measures, it is very important to enhance the adaptability capacity [39]. For example, Shun Y et al. pointed out that the impact of public infrastructure, insurance protection, medical services, etc., is highlighted in the adaptive indicators, and most of the adaptive indicators can be improved in the short term [16]. Therefore, it is very necessary to improve adaptability indicators to alleviate regional vulnerability.

5.3. Suggestions for Disaster Prevention and Mitigation of Storm Surges in China

This paper analyzes the temporal and spatial changes in the vulnerability of different types of coastal city in China, along with the intrinsic link between economic development and vulnerability, to help plan and reduce disaster-related costs. First, we highlighted the temporal and spatial development laws of different types of city in coastal areas, and then we further analyzed the main influencing factors that affect the development laws of vulnerability. The results show that the vulnerability of different types of city shows a declining development law, and that the coastal vulnerability can be greatly alleviated by improving the adaptability index. It is suggested that, when reducing the vulnerability of coastal cities, relevant departments should give priority to agricultural cities and northern cities with moderate urbanization development, such as Binzhou and Tianjin. For some coastal cities in China with relatively average economic development, the post-disaster recovery costs are high, and resilience is low. Coastal areas should pay attention to economic development. Furthermore, in Shenzhen and Dongguan, the vulnerability of the two cities rapidly decreased due to the increase in the proportion of investment in adaptation-related resources by relevant government departments. According to the discussion in Section 5.1, Shenzhen and Dongguan are at high risk of storm surge damage. With global warming, regions above sea level, and even the entire coast of China, may experience stronger storm damage in the future [40,41], which may aggravate the risk of direct economic losses in coastal cities. Therefore, not only Shenzhen and Dongguan, but all of the coastal cities in China, need to continuously increase their ability to adapt to disasters while developing the economy, thereby reducing the cost of future disaster losses.

5.4. Limitation and Uncertainty of Assessment

In the face of storm surge disasters in coastal areas, urban vulnerability changes have spatiotemporal characteristics. Therefore, this paper analyzes the spatiotemporal changes in the vulnerability of 15 coastal cities in China from 1990 to 2020 and further reveals the relationship between economic development and vulnerability changes. The results of the paper show that the city's adaptability to disasters has the highest correlation with vulnerability, and the degree of urban vulnerability decreases with the increase in adaptability. From the perspective of economic development, this paper explores the changes in urban vulnerability in the face of storm surge disasters and concludes that the main reason for the continuous reduction in the vulnerability of coastal cities from 1990 to 2020 was the continuous improvement in urban adaptability. In this research, the adaptability of coastal cities was evaluated based on the general public budget expenditure, investment in fixed assets, GDP, and other indicators in urban statistical data. Although the urban statistical indicators have a high temporal coherence, the change in adaptability at a finer scale was assessed. Existing statistical indicators are far from explanatory, so it is necessary to develop long-term adaptation data at finer scales for a dynamic assessment of coastal vulnerability.

A combination of factors can increase the vulnerability of coastal areas. For example, global warming can lead to sea level rises in coastal areas, increasing the risk of inundation of fragile coastal areas, such as coastal cities and deltas that were originally low-lying plains. Frequent occurrences will increase the vulnerability of coastal areas. In addition to the abovementioned uncontrollable disaster factors, the increase in the proportion of children and the elderly in coastal areas, as well as the increase in fishing intensity and other sensitive indicators, will also increase the vulnerability. Therefore, in future research, in addition to overcoming the limitations of the lack of long-term fine-scale data, more attention should be paid to the temporal and spatial variation laws of coastal vulnerability in highly exposed and highly sensitive coastal cities, deltas, and other regions, and intrinsic drivers of vulnerability changes in those areas should be further studied.

6. Conclusions

Previous studies of the vulnerability to storm surge disasters in China have focused on the spatial distribution characteristics of vulnerability and neglected the temporal and spatial changes in the vulnerability of different types of coastal city in China, as well as the relationship between economic development and vulnerability. Therefore, this paper analyzes the temporal and spatial variation characteristics and differences in vulnerability in 15 typical coastal cities in China from 1990 to 2020 and further explores the relationships between urban exposure, adaptability, sensitivity, and vulnerability. This paper also aimed to reveal the impact of the accelerated urbanization process of economic development on the changes in vulnerability in coastal areas, as well as to provide a scientific basis for improving the comprehensive disaster reduction ability with respect to storm surge disasters and coping with storm surge disaster risks in China's coastal areas.

The results show that the vulnerability declined the fastest from 2005 to 2015, and that the areas with the highest vulnerability shifted from the southern region to the northern region. The southern cities of Shanghai, Shenzhen, and Dongguan had low vulnerability values and high risk resistance ability when facing storm surge disasters. The improvement in economic capacity greatly improved cities' ability to adapt to disasters, and the improvements in adaptability greatly contributed to the reduction in urban vulnerability. Furthermore, this article further reveals that the general public budget expenditure capacity, investment in fixed assets, GDP, and healthcare level can effectively alleviate the city's vulnerability, with the help of exposure and sensitivity. The effect of vulnerability is not significant, but the vulnerability of cities in the face of storm surge disasters can be alleviated by controlling the speed of exposure and sensitivity increases through effective means. Finally, we should note that, due to the frequent storm surge disasters in cities during the 2005–2015 period, government departments strengthened the input of relevant resources in the adaptive capacity, ultimately meaning that the cities' vulnerability declined faster during this period.

In future research, it will be necessary to develop long-term adaptive index data at a finer scale, and to pay more attention to the temporal and spatial variation patterns of vulnerability in coastal cities, deltas, and other high-exposure and high-sensitivity coastal areas. It will also be necessary to deeply study the impact of internal drivers of vulnerability changes in high-exposure and high-sensitivity areas. Furthermore, more consideration should be given to the coastal attributes related to natural disasters of the storm surge type in the exposure indicators in future studies—such as relief, landform, rock type, ocean vertical movement, tidal range, wave height, shoreline displacement rate, coastal slope, relative SLR rate, shoreline erosion/acceleration rate, barrier type, beach type, storm surge wave climb, sediment granularity, hinterland nature, coastal elevation, coastal land use, foreshore width, presence of vegetation, presence of manmade or natural protection, shape state restoring force, etc.—and the collection of related data on the time dynamic index for comparative study.

Author Contributions: Conceptualization, X.Y. and Y.L.; methodology, Y.L.; software, X.L.; validation, D.M., X.L. and J.Z.; formal analysis, D.M.; investigation, X.Y.; resources, K.G.; data curation, D.M.; writing—original draft preparation, D.M.; writing—review and editing, D.M.; visualization, X.Y.; supervision, Z.W.; project administration, X.Y.; funding acquisition, X.Y. All authors have read and agreed to the published version of the manuscript.

Funding: This research was funded by the Earth Big Data Science Project of CAS (XDA19060202), the National Key Research and Development Program of China (Grant No. 2021YFB3900501), and the Innovation Project of LREIS (Grant No. O88RAA01YA).

Institutional Review Board Statement: Not applicable.

Informed Consent Statement: Not applicable.

Data Availability Statement: Not applicable.

Conflicts of Interest: The authors declare no conflict of interest. The funders had no role in the design of the study; in the collection, analyses, or interpretation of data; in the writing of the manuscript; or in the decision to publish the results.

Appendix A

A total of five schedules are cited in the text—Table A1: GLC_FCS30 land cover classification system. Table A2: The annual mean change rate of sensitivity indicators in 15 coastal cities from 1990 to 2020. Table A3: The annual mean change rate of adaptability index in 15 coastal cities from 1990 to 2020. Table A4: The results of vulnerability and the change rate of each stage in 15 coastal cities from 1990 to 2020. Table A5: The weight values and vulnerability correlation values of the adaptability index of 15 coastal cities. Details of the tables are shown in Appendix A.

Table A1. GLC_FCS30 land cover classification system.

LC id	Classification System	Exposure Value
10	Rainfed cropland	0.8
11	Herbaceous cover	0.4
12	Tree or shrub cover (Orchard)	0.4
20	Irrigated cropland	0.8
51	Open evergreen broadleaved forest	0.4
52	Closed evergreen broadleaved forest	0.4
61	Open deciduous broadleaved forest (0.15 < fc < 0.4)	0.4
62	Closed deciduous broadleaved forest (fc > 0.4)	0.4
71	Open evergreen needle-leaved forest (0.15 < fc < 0.4)	0.4
72	Closed evergreen needle-leaved forest (fc > 0.4)	0.4
81	Open deciduous needle-leaved forest (0.15 < fc < 0.4)	0.4
82	Closed deciduous needle-leaved forest (fc > 0.4)	0.4
91	Open mixed-leaf forest (broadleaved and needle-leaved)	0.4
92	Closed mixed-leaf forest (broadleaved and needle-leaved)	0.4
120	Shrubland	0.4
121	Evergreen shrubland	0.4
122	Deciduous shrubland	0.4
130	Grassland	0.4
140	Lichens and mosses	0.4
150	Sparse vegetation (fc < 0.15)	0.4
152	Sparse shrubland (fc < 0.15)	0.4
153	Sparse herbaceous (fc < 0.15)	0.4
180	Wetlands	0.6
190	Impervious surfaces	1
200	Bare areas	0.2
201	Consolidated bare areas	0.2
202	Unconsolidated bare areas	0.2
210	Water body	0.2
220	Permanent ice and snow	0
250	Filled value	0

Table A2. Annual mean change rate of sensitivity indicators in 15 coastal cities from 1990 to 2020.

City	C1 (%/Year)	C2 (10,000 People/Year)	C3 (%/Year)	C4 (%/Year)
Shanghai	−0.0003	1.10	−0.0014	−0.0003
Guangzhou	−0.0004	7.08	−0.0023	−0.0001
Shenzhen	−0.0017	5.28	−0.0017	−0.0006
Tianjin	0.0004	1.84	−0.0029	−0.0004
Weifang	0.0000	0.57	−0.0086	−0.0003
Yancheng	0.0003	−0.76	−0.0116	−0.0016
Zhanjiang	0.0001	1.13	−0.0074	−0.0021
Hangzhou	−0.0001	2.76	−0.0051	−0.0015
Zhongshan	−0.0012	1.35	−0.0097	−0.0002
Binzhou	0.0000	1.55	−0.0062	−0.0004
Huizhou	−0.0010	2.32	−0.0103	−0.0005
Dongguan	−0.0031	3.96	−0.0075	−0.0067
Fuzhou	0.0002	1.81	−0.0077	0.0011
Weihai	0.0000	0.19	−0.0114	−0.0021
Dalian	0.0005	0.68	−0.0022	−0.0011

Table A3. The annual mean change rate of adaptability index in 15 coastal cities from 1990 to 2020.

City	B1 (Million CNY/Year)	B2 (Million CNY/Year)	B3 (CNY/Year)	B4 (CNY/Year)	B5 (Million CNY/Year)	B6 (1000 Persons/Year)	B7
Shanghai	278.51	1415.67	2674.91	1228.53	294.58	2.70	−46
Guangzhou	97.61	823.32	2185.17	990.90	250.68	5.54	107
Shenzhen	138.62	917.81	2025.02	791.23	264.15	4.11	163
Tianjin	66.97	459.45	1534.00	820.73	522.92	1.55	81
Weifang	26.15	190.93	1384.50	696.23	156.95	1.87	238
Yancheng	32.22	195.02	1297.17	758.30	142.34	1.06	82
Zhanjiang	17.74	100.15	1022.59	597.84	54.37	1.31	99
Hangzhou	68.59	530.93	2222.70	1250.97	257.12	0.67	131
Zhongshan	12.44	103.60	1711.34	1181.16	43.86	0.91	30
Binzhou	14.89	82.21	1234.00	600.00	49.96	0.68	30
Huizhou	21.10	139.10	1429.08	793.14	80.95	1.33	99
Dongguan	27.94	319.52	1851.46	1242.83	79.95	2.19	102
Fuzhou	31.44	330.59	1579.73	726.83	178.55	1.48	125
Weihai	11.56	98.37	1628.07	745.17	91.81	0.63	72
Dalian	32.75	228.39	1519.02	685.13	54.13	1.42	99

Table A4. The results of vulnerability and the change rate of each stage in 15 coastal cities from 1990 to 2020.

City	1990	1990–1995 (%)	1995	1995–2000 (%)	2000	2000–2005 (%)	2005	2005–2010 (%)	2010	2010–2015 (%)	2015	2015–2020 (%)	2020
Shanghai	0.80	−2.70	0.67	−1.45	0.59	−1.42	0.52	−1.78	0.43	−2.44	0.31	−3.46	0.14
Guangzhou	0.75	0.16	0.76	−1.70	0.67	−1.69	0.59	−2.32	0.47	−2.40	0.35	−2.90	0.20
Shenzhen	0.84	−5.80	0.56	−1.02	0.50	−2.32	0.39	−0.15	0.38	−2.78	0.24	−1.00	0.19
Tianjin	0.70	0.10	0.71	−1.47	0.63	−0.99	0.58	−2.62	0.45	−3.95	0.25	0.46	0.28
Weifang	0.77	−0.09	0.77	−1.11	0.71	−3.15	0.56	−2.06	0.45	−3.93	0.26	−0.67	0.22
Yancheng	0.71	1.88	0.80	0.19	0.81	−3.46	0.64	−3.60	0.46	−4.32	0.24	−1.92	0.14
Zhanjiang	0.76	−0.60	0.73	−0.71	0.70	−1.21	0.64	−1.48	0.56	−6.15	0.26	−1.18	0.20
Hangzhou	0.74	−2.16	0.63	−0.75	0.59	−1.12	0.54	−1.03	0.48	−2.23	0.37	−2.69	0.24
Zhongshan	0.78	−1.97	0.69	−1.66	0.60	−1.76	0.51	−2.00	0.41	−2.87	0.27	−1.73	0.18
Binzhou	0.64	0.39	0.66	0.90	0.71	−1.73	0.62	−3.17	0.46	−1.42	0.39	−1.10	0.33
Huizhou	0.79	−2.29	0.67	−0.70	0.64	−1.38	0.57	−2.69	0.43	−2.44	0.31	−1.89	0.22
Dongguan	0.85	−3.12	0.69	−2.36	0.57	−2.62	0.44	−2.15	0.33	−0.84	0.29	−2.67	0.16
Fuzhou	0.78	−2.15	0.67	−0.22	0.66	−1.05	0.61	−2.05	0.51	−3.43	0.33	−2.51	0.21
Weihai	0.75	−1.28	0.68	−1.31	0.62	−2.09	0.51	−2.66	0.38	−2.06	0.28	−1.24	0.21
Dalian	0.73	−1.04	0.68	−0.58	0.65	−1.88	0.56	−3.57	0.38	−0.90	0.33	−0.12	0.33

Table A5. The weight values and vulnerability correlation values of the adaptability index of 15 coastal cities.

City Name	CWM Weight Value							Pearson's Correlation Coefficient						
	B1	B2	B3	B4	B5	B6	B7	B1	B2	B3	B4	B5	B6	B7
Shanghai	0.08	0.08	0.08	0.07	0.07	0.04	0.05	0.96 **	0.97 **	0.97 **	0.96 **	0.99 **	0.61	−0.16
Guangzhou	0.08	0.08	0.07	0.07	0.08	0.06	0.05	0.97 **	0.99 **	0.99 **	0.98 **	0.99 **	0.95 **	0.88 **
Shenzhen	0.07	0.06	0.05	0.05	0.06	0.05	0.05	0.81 *	0.82 *	0.90 **	0.93 **	0.76 *	0.81 *	0.85 *
Tianjin	0.08	0.09	0.07	0.07	0.09	0.04	0.05	0.96 **	0.99 **	0.96 **	0.95 **	0.97 **	0.80 *	0.78 *
Weifang	0.09	0.08	0.07	0.07	0.10	0.07	0.09	0.96 **	0.99 **	0.97 **	0.97 **	0.99 **	0.97 **	0.90 **
Fuzhou	0.10	0.08	0.07	0.07	0.10	0.05	0.06	0.97 **	0.97 **	0.99 **	0.99 **	0.97 **	0.96 **	0.84 *
Hangzhou	0.08	0.08	0.07	0.07	0.08	0.04	0.05	0.95 **	0.97 **	0.98 **	0.97 **	0.96 **	0.65	0.94 **
Zhongshan	0.09	0.09	0.06	0.06	0.08	0.06	0.06	0.94 **	0.97 **	0.97 **	0.94 **	0.98 **	0.96 **	0.93 **
Binzhou	0.07	0.07	0.06	0.07	0.07	0.05	0.07	0.96 **	0.97 **	0.95 **	0.94 **	0.69	0.97 **	0.92 **
Huizhou	0.08	0.07	0.06	0.07	0.08	0.06	0.08	0.94 **	0.97 **	0.98 **	0.95 **	0.96 **	0.93 **	0.97 **
Dongguan	0.07	0.07	0.06	0.06	0.06	0.06	0.07	0.88 **	0.91 **	0.97 **	0.95 **	0.92 **	0.90 **	0.93 **
Weihai	0.09	0.08	0.06	0.06	0.08	0.05	0.09	0.96 **	0.99 **	0.96 **	0.96 **	0.96 **	0.98 **	0.90 **
Dalian	0.10	0.09	0.08	0.08	0.10	0.05	0.05	0.97 **	0.98 **	0.93 **	0.96 **	0.85 *	0.82*	0.87*
Zhanjiang	0.09	0.08	0.07	0.07	0.09	0.06	0.09	0.99 **	0.99 **	0.97 **	0.98 **	0.99 **	0.98 *	0.98**
Yancheng	0.09	0.08	0.07	0.07	0.09	0.05	0.09	0.97 **	0.97 **	0.97 **	0.96 **	0.99 **	0.93 **	0.96 **

*, ** mean the result at 10% and 5% significance level respectively.

References

1. Cai, F.; Cao, C.; Qi, H.S.; Su, X.Z.; Lei, G.; Liu, J.H.; Zhao, S.H.; Liu, G.; Zhu, K. Rapid migration of mainland China's coastal erosion vulnerability due to anthropogenic changes. *J. Environ. Manage.* **2022**, *319*, 15. [CrossRef] [PubMed]
2. Bagdanaviciute, I.; Kelpsaite, L.; Soomere, T. Multi-criteria evaluation approach to coastal vulnerability index development in micro-tidal low-lying areas. *Ocean Coast. Manag.* **2015**, *104*, 124–135. [CrossRef]
3. Kantamaneni, K. Counting the cost of coastal vulnerability. *Ocean Coastal. Manag.* **2016**, *132*, 155–169. [CrossRef]
4. Yin, J.; Yin, Z.; Xu, S. Composite risk assessment of typhoon-induced disaster for China's coastal area. *Nat. Hazards* **2013**, *69*, 1423–1434. [CrossRef]
5. Fang, J.; Lincke, D.; Brown, S.; Nicholls, R.J.; Wolff, C.; Merkens, J.-L.; Hinkel, J.; Vafeidis, A.T.; Shi, P.; Liu, M. Coastal flood risks in China through the 21st century—An application of DIVA. *Sci. Total Environ.* **2020**, *704*, 135311. [CrossRef]
6. The State Council the People's Republic of China. Available online: http://www.gov.cn/zhengce/zhengceku/2022-07/22/content_5702154.htm (accessed on 25 December 2022).
7. Roukounis, C.N.; Tsihrintzis, V.A. Indices of Coastal Vulnerability to Climate Change: A Review. *Environ. Process.* **2022**, *9*, 29. [CrossRef]
8. Shi, X.; Han, Z.; Fang, J.; Tan, J.; Guo, Z.; Sun, Z. Assessment and zonation of storm surge hazards in the coastal areas of China. *Nat. Hazards* **2019**, *100*, 39–48. [CrossRef]
9. Sajjad, M.; Chan, J.C.L.; Kanwal, S. Integrating spatial statistics tools for coastal risk management: A case-study of typhoon risk in mainland China. *Ocean Coastal. Manag.* **2020**, *184*, 14. [CrossRef]
10. Xu, X.; Sun, D.; Guo, T. A systemic analysis of typhoon risk across China. *Nat. Hazards* **2015**, *77*, 461–477. [CrossRef]
11. Wang, S.F.; Wang, W.A.; Ji, M.H.; Chen, W.; Xu, S.Y. Assessment of Vulnerability to Sea-level Rise for China's Coast. In Proceedings of the 21st International Conference on Geoinformatics (Geoinformatics), Kaifeng, China, 20–22 June 2013.
12. Yin, J.; Xu, S.; Wang, J.; Zhong, H. Vulnerability Assessment of Combined Impacts of Sea Level Rise and Coastal Flooding for China's Coastal Region Using Remote Sensing and GIS. In Proceedings of the 18th International Conference on Geoinformatics: GIScience in Change, Geoinformatics 2010, Peking University, Beijing, China, 18–20 June 2010.
13. Wang, Y.X.; Guo, Z.X.; Zheng, S.X.; Zhang, M.; Shu, X.J.; Luo, J.; Qiu, L.G.; Gao, T. Risk assessment for typhoon-induced storm surges in Wenchang, Hainan Island of China. *Geomat. Nat. Hazards Risk* **2021**, *12*, 880–899. [CrossRef]
14. Shi, X.; Qiu, J.; Chen, B.; Zhang, X.; Guo, H.; Wang, J.; Bei, Z. Storm surge risk assessment method for a coastal county in China: Case study of Jinshan District, Shanghai. *Stoch. Environ. Res. Risk Assess.* **2020**, *34*, 627–640. [CrossRef]
15. Liu, Q.; Ruan, C.; Zhong, S.; Li, J.; Yin, Z.; Lian, X. Risk assessment of storm surge disaster based on numerical models and remote sensing. *Int. J. Appl. Earth Obs. Geoinf.* **2018**, *68*, 20–30. [CrossRef]
16. Yuan, S.; Guo, J.; Zhao, X. Integrated Weighting Technique for Coastal Vulnerability to Storm Surges. *J. Coast. Res.* **2017**, *80*, 6–12. [CrossRef]
17. Gao, Y.; Wang, H.; Liu, G.M.; Sun, X.Y.; Fei, X.Y.; Wang, P.T.; Lv, T.T.; Xue, Z.S.; He, Y.W. Risk assessment of tropical storm surges for coastal regions of China. *J. Geophys. Res.-Atmos.* **2014**, *119*, 5364–5374. [CrossRef]
18. Moser, S.C.; Jeffress Williams, S.; Boesch, D.F. Wicked Challenges at Land's End: Managing Coastal Vulnerability Under Climate Change. *Annu. Rev. Environ. Resour.* **2012**, *37*, 51–78. [CrossRef]
19. Li, C.; Yu, Z.; Yuan, Y.; Geng, X.; Zhang, D.; Zheng, X.; Li, R.; Sun, W.; Wang, X. A synthetic water-heat-vegetation biodiversity nexus approach to assess coastal vulnerability in eastern China. *Sci. Total Environ.* **2022**, *845*, 157074. [CrossRef]
20. Zhou, Y.; Pu, L.; Zhu, M. Coastal Landscape Vulnerability Analysis in Eastern China—Based on Land-Use Change in Jiangsu Province. *Int. J. Environ. Res. Public Health* **2020**, *17*, 1702. [CrossRef]
21. Yu, H.; Shen, Y.; Kelly, R.M.; Qi, X.; Wu, K.; Li, S.; Yu, H.; Bao, X. Trends in social vulnerability to storm surges in Shenzhen, China. *Nat. Hazards Earth Syst. Sci.* **2020**, *20*, 2447–2462. [CrossRef]
22. Zhao, Q.L.; Xu, S.Y.; Wang, J.; Hu, B.B.; Ye, M.W. A review of risk assessment of storm surge on coastal cities. *Prog. Geogr.* **2007**, *5*, 34–42. [CrossRef]
23. Liu, L.; Zhang, X.; Gao, Y.; Chen, X.; Shuai, X.; Mi, J. Finer-Resolution Mapping of Global Land Cover: Recent Developments, Consistency Analysis, and Prospects. *J. Remote Sens.* **2021**, *2021*, 1–38. [CrossRef]
24. Rizzi, J.; Torresan, S.; Zabeo, A.; Critto, A.; Tosoni, A.; Tomasin, A.; Marcomini, A. Assessing storm surge risk under future sea-level rise scenarios: A case study in the North Adriatic coast. *J. Coast. Conserv.* **2017**, *21*, 453–471. [CrossRef]
25. Liu, Y.; Lu, C.; Yang, X.; Wang, Z.; Liu, B. Fine-Scale Coastal Storm Surge Disaster Vulnerability and Risk Assessment Model: A Case Study of Laizhou Bay, China. *Remote Sens.* **2020**, *12*, 1301. [CrossRef]
26. Arun Kumar, A.; Kunte, P.D. Coastal vulnerability assessment for Chennai, east coast of India using geospatial techniques. *Nat. Hazards* **2012**, *64*, 853–872. [CrossRef]
27. Balica, S.F.; Wright, N.G.; van der Meulen, F. A flood vulnerability index for coastal cities and its use in assessing climate change impacts. *Nat. Hazards* **2012**, *64*, 73–105. [CrossRef]
28. Li, A.; Ismail, A.B.; Thu, K.; Ng, K.C.; Loh, W.S. Performance evaluation of a zeolite–water adsorption chiller with entropy analysis of thermodynamic insight. *Appl. Energy* **2014**, *130*, 702–711. [CrossRef]
29. Lai, D.; Sun, W.; Pan, W.; Linder, S.H. Application of principal component analysis on human development indicators: Temporal approach from 1999 to 2010. *Int. J. Disabil. Hum. Dev.* **2014**, *13*, 97–103. [CrossRef]

30. Peng, Z. Zong He Ping Jia Guo Cheng Zhong de Xiang Guan Wen Ti Fang Fa Yan Jiu. Hefei University of Technology. 2015. Available online: https://kns.cnki.net/KCMS/detail/detail.aspx?dbname=CDFDLAST2016&filename=1015723314.nh (accessed on 5 January 2023).
31. Valencia, D.; Lillo, R.E.; Romo, J. A Kendall correlation coefficient between functional data. *Adv. Data Anal. Classif.* **2019**, *13*, 1083–1103. [CrossRef]
32. Yuan, S.; Zhao, X.; Li, L. JIYURST-CWMMOXINGDEFENGBAOCHAOZAIHAICUIRUOXINGZUHEPINGJIA. *Stat. Decis.* **2015**, *23*, 53–56. [CrossRef]
33. Ministry of Natural Resources of the People's Republic of China. Available online: https://www.mnr.gov.cn/sj/sjfw/hy/gbgg/zghyzhgb/ (accessed on 25 October 2022).
34. Hoque, M.A.-A.; Pradhan, B.; Ahmed, N.; Ahmed, B.; Alamri, A.M. Cyclone vulnerability assessment of the western coast of Bangladesh. *Geomat. Nat. Hazards Risk* **2021**, *12*, 198–221. [CrossRef]
35. Mafi-Gholami, D.; Zenner, E.K.; Jaafari, A.; Riyahi Bakhtyari, H.R.; Tien Bui, D. Multi-hazards vulnerability assessment of southern coasts of Iran. *J. Environ. Manag.* **2019**, *252*, 109628. [CrossRef]
36. Helderop, E.; Grubesic, T.H. Hurricane storm surge in Volusia County, Florida: Evidence of a tipping point for infrastructure damage. *Disasters* **2019**, *43*, 157–180. [CrossRef] [PubMed]
37. Tragaki, A.; Gallousi, C.; Karymbalis, E. Coastal Hazard Vulnerability Assessment Based on Geomorphic, Oceanographic and Demographic Parameters: The Case of the Peloponnese (Southern Greece). *Land* **2018**, *7*, 56. [CrossRef]
38. Li, K.; Li, G.S. Risk assessment on storm surges in the coastal area of Guangdong Province. *Nat. Hazards* **2013**, *68*, 1129–1139. [CrossRef]
39. Hoque, M.A.-A.; Phinn, S.; Roelfsema, C.; Childs, I. Assessing tropical cyclone risks using geospatial techniques. *Appl. Geogr.* **2018**, *98*, 22–33. [CrossRef]
40. Lok, C.C.F.; Chan, J.C.L. Changes of tropical cyclone landfalls in South China throughout the twenty-first century. *Clim. Dyn.* **2017**, *51*, 2467–2483. [CrossRef]
41. Mei, W.; Xie, S.-P. Intensification of landfalling typhoons over the northwest Pacific since the late 1970s. *Nat. Geosci.* **2016**, *9*, 753–757. [CrossRef]